Published OnlineFirst January 26, 2010; DOI: 10.1158/0008-5472.CAN-09-3662

for tumor progression. Therefore, a species-matched (murine) microenvironment is needed to examine the nature of cells strongly expressing PSF1.

Here, we have investigated the expression of PSF1 and the localization of PSF1-positive cancer cells in a mouse tumor cell xenograft model. We observed malignant behavior of highly PSF1-positive tumor cells with regard to tumorigenesis and metastasis. Moreover, highly PSF1-positive cancer cells have been characterized by microarray analysis, and the data compared with those of the recently reported embryonic stem cell (ESC)–like gene expression signature in poorly differentiated aggressive human tumors (18). Finally, to determine whether PSF1 could be a molecular target for the development of anticancer drugs, we silenced the *PSF1* gene by the RNA interference (RNAi) method in human carcinoma cell lines and observed the effects thereof on the growth of the cancer cells.

Materials and Methods

Cell culture and cell line construction. LLC, B16, NIH3T3, HeLa, and HEK293T were maintained in DMEM (Sigma) with 10% fetal bovine serum (FBS; Sigma) and penicillin/streptomycin (Life Technologies, Inc.). Colon26 cells were maintained in RPMI 1640 (Sigma) with 10% FBS and penicillin/streptomycin. Mouse embryonic fibroblasts were prepared from day 14.5 embryos and cultured in high-glucose DMEM (Sigma) with 10% FBS and penicillin/streptomycin.

The gene encoding the PSF1 promoter region was isolated by mouse BAC cloning (RP23-193L22, Advanced GenoTechs Co.). Using the 5′ upstream sequence of the first exon of the *PSF1* locus as a probe, 5.5 kb of the 5′flanking PSF1 gene were isolated and subcloned into pBluescript II KS (Stratagene). The enhanced green fluorescent protein (*EGFP*) gene and the *neomycin* gene were excised from pEGFP-N1 and pcDNA3.1(−) (Clontech), respectively, and ligated to the 5.5 kb of the PSF1 5′-flanking fragment. This construct was designated *PSF1p-EGFP*. LLC and colon26 cells were transfected using Lipofectamine 2000 (Invitrogen). After transfection, the cells were cultured in medium supplemented with G418 (Life Technologies) to obtain cells stably expressing EGFP under the control of the PSF1 promoter (LLC-*PSF1p-EGFP* and colon26-*PSF1p-EGFP*).

Quantitative reverse transcription-PCR. Quantitative reverse transcription-PCR (RT-PCR) was done as previously described (14). The primer sets were described in Supplementary Materials and Methods.

Mice. Seven- to eight-week-old C57BL/6 female mice (for the LLC experiments) and BALB/c female mice of the same age (for colon26) were purchased from Japan SLC. All animal studies were approved by the Osaka University Animal Care and Use Committee. Subcutaneous xenografts were established by injecting 10^6 cells into the flanks of the mice.

Flow cytometric analysis. Single-cell suspensions from tumors were prepared using a standard protocol. Cell sorting was done using a FACSAria (Becton Dickinson). For the EGFP^{high} population, the 5% most brightly fluorescing cells were sorted, and for the EGFP^{low} population, the 5% least fluorescent. We used parental LLC or colon26 as negative controls.

In vitro *clonal analyses and* in vivo *tumorigenicity analysis.* Isolated cells were plated on 10-cm culture dishes (200 per dish for LLC-*PSF1p-EGFP* and 100 per dish for colon26-*PSF1p-EGFP*) and cultured. The percentage of cells that initiated a clone was taken as the plating efficiency. For *in vivo* experiments, 100 sorted cells in 100 μL of PBS with growth factor–reduced Matrigel (BD Biosciences; 1:1) were injected s.c. into the mice. Five weeks after injection, tumor volumes were measured with a caliper and calculated as width × width × length × 0.52.

Invasion assay and metastasis assay. The invasive activity of tumor cells was assayed using a BioCoat Matrigel Invasion Chamber (BD Biosciences) according to the manufacturer's instruction.

For the lung metastasis assay using LLC-*PSF1p-EGFP*, 10^5 viable sorted cells were injected into the tail veins of mice. After 4 wk, lungs were dissected and the number of colonies observable on the surface of the lungs was noted. For the hepatic metastasis assay of colon26-*PSF1p-EGFP*, spleens of mice were exposed to allow the direct injection of 5×10^4 viable sorted cells. After 12 d, livers and spleens were dissected out and the number of colonies observable on the surface of the livers was recorded. Sections of liver were stained with H&E to evaluate tissue morphology and to detect metastases.

Immunohistochemistry and immunocytochemistry. Immunohistochemical analyses were done as previously described (19). Rabbit anti-GFP antibody (Invitrogen) and rat anti-CD31 (BD Biosciences) were used for primary antibodies. For the fluorescent immunohistochemical analyses, phycoerythrin-conjugated anti-CD31 (BD Biosciences) was used for staining endothelial cells.

For immunocytochemistry, anti-PSF1(14), anti-bromodeoxyuridine (BrdUrd) (Zymed Laboratories), anti-β-tubulin (Sigma), anti–CENP-A (MBL), and anti-survivin (Chemicon International, Inc.) antibodies were used as previously described (14).

PSF1 *knockdown.* Transfection was done using Lipofectamine 2000 (Invitrogen). For the enrichment of transiently shRNA vector–transfected cells, the puromycin resistance gene was ligated into the *Xho*I site of the pSINsi-hU6 vector (Takara), and then sense and antisense oligonucleotide pairs (see below) were annealed and ligated into the *Bam*HI/*Cla*I site of the pSINsi-hU6-P vectors. The sequences of the oligonucleotide sets were described in Supplementary Materials and Methods. For time-lapse imaging of histone H3 and tubulin in living cells, HEK293T cells were transfected with GFP-histone (20) or tubulin-GFP (Clontech) expression vectors, and stably expressing clones were selected. Time-lapse observation was done as previously reported using an IX70 microscope (Olympus; ref. 21).

Microarray and bioinformatics analysis. Microarrays were done as previously described (22). Raw data are available for download from GEO (GSE17112). Gene set enrichment analysis (GSEA; ref. 23) was done by CeresBioscience as previously reported.

Statistical analysis. Results were expressed as the mean ± SEM. Student's *t* test was used for statistical analysis. Differences were considered statistically significant when $P < 0.01$.

Published OnlineFirst January 26, 2010; DOI: 10.1158/0008-5472.CAN-09-3662

Results

Establishment of transgenic cell lines to monitor endogenous* PSF1 *expression in living cells. We first examined *PSF1* mRNA expression in mouse cancer cell lines, a noncancer cell line, and primary cultured cells. *PSF1* mRNA in cancer cell lines is expressed to a greater degree than in the noncancer cell line or primary cultured cells (Fig. 1A). To determine whether the cancer cells strongly expressing PSF1 had malignant features, they need to be collected as living cells. Because PSF1 is an intracellular protein, viable cells cannot be isolated using PSF1 antibody and flow cytometric cell sorting. Therefore, we used promoter activity to monitor the expression level of PSF1 in cancer cells in the murine tumor xenograft model. We have cloned the mouse *PSF1* promoter gene and established lung carcinoma [Lewis lung carcinoma (LLC)] and colon cancer (colon26) cell lines stably expressing EGFP under the transcriptional control of the *PSF1* promoter (LLC- and colon26-*PSF1p-EGFP*, respectively). We confirmed *PSF1* mRNA expression in parental LLC and colon26 cells (data not shown). After inoculation of LLC-*PSF1p*-EGFP, tumors were dissected and the intensity of EGFP in dissociated cancer cells was analyzed by flow cytometry (Fig. 1B–D). As can be seen, EGFP-positive ($EGFP^+$) cells containing high or low levels of EGFP ($EGFP^{high}$ or $EGFP^{low}$ cells, respectively) were present. These were separated and the expression of *PSF1* mRNA was examined (Fig. 1D). The results indicate that the intensity of EGFP is correlated with the endogenous *PSF1* expression. Similar results were obtained using colon26-*PSF1p-EGFP* (data not shown). These results suggest that these cell lines are useful tools to monitor endogenous *PSF1* expression in living cells.

EGFP(PSF1)^{high} cells possess greater tumorigenic capacity. To study their colony forming efficiency, cancer cells

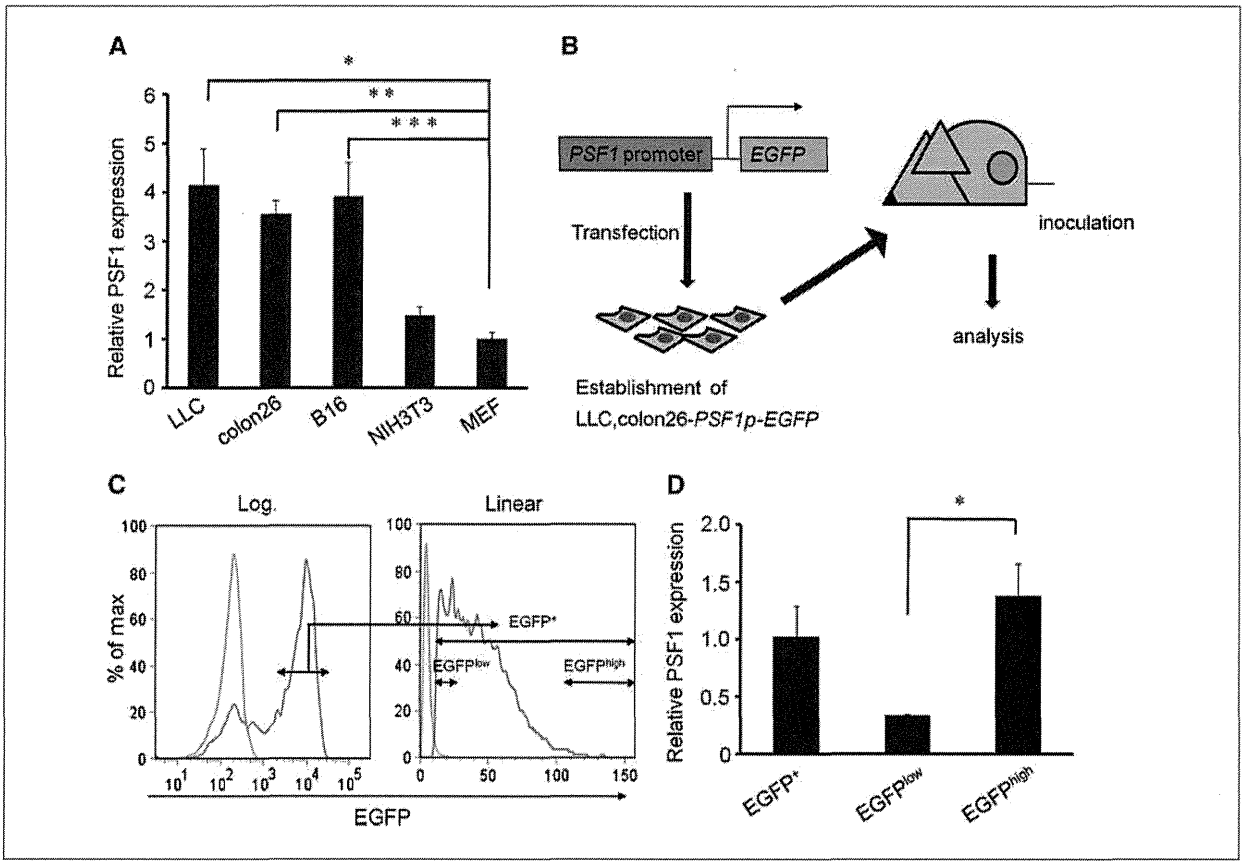

Figure 1. PSF1 expression in murine carcinoma cell lines. A, expression of *PSF1* mRNA in murine carcinoma cells. Total RNA was analyzed by quantitative RT-PCR for *PSF1* expression in different murine carcinoma cell lines and compared with a noncancer cell line and a primary cell culture. The values are normalized to the amount of mRNA in mouse embryonic fibroblasts. *LLC*, lung carcinoma; *colon26*, colon carcinoma; *B16*, melanoma; *NIH3T3*, mouse embryonic fibroblast cell line; *MEF*, mouse embryonic fibroblast. Data show the mean ± SEM. *, **, ***, $P < 0.01$ ($n = 3$). B, experimental procedure. We have cloned the mouse *PSF1* promoter gene and established cell lines stably expressing EGFP under the transcriptional control of the *PSF1* promoter (LLC- and colon26-*PSF1p-EGFP*, respectively). After inoculation of LLC- or colon26-*PSF1p*-EGFP, tumors were dissected and the dissociated cancer cells were separated using a cell sorter according to the intensity of EGFP expression and further analyzed. C, fluorescence-activated cell sorting analysis of cells from tumor tissues injected with LLC (green) or LLC-*PSF1p-EGFP* (red) cells. $EGFP^+$, $EGFP^{low}$, and $EGFP^{high}$ cells were sorted as indicated. Intensity of EGFP is displayed on a log or linear scale. D, quantitative RT-PCR analysis of *PSF1* mRNA expression in sorted cells as indicated. The values are normalized to the amount of mRNA in $EGFP^+$ cells. Data show the mean ± SEM. *, $P < 0.01$ ($n = 3$).

Published OnlineFirst January 26, 2010; DOI: 10.1158/0008-5472.CAN-09-3662

(LLC- and colon26-*PSF1p-EGFP*) from tumor-bearing mice were divided into three fractions (EGFP$^+$, EGFP^{low}, and EGFP^{high}) as indicated in Fig. 1C, seeded, and cultured for 2 weeks. EGFP^{high} cells formed significantly larger colonies than did EGFP^{low} cells (Fig. 2A) in both colon26 and LLC tumors.

We next examined the serial transplantation ability of these cells. We inoculated sorted EGFP^{high} or EGFP^{low} cells from tumor-bearing mice into new hosts to evaluate the relationship between PSF1 expression and tumorigenicity. Four weeks (LLC-*PSF1p-EGFP*) or 2 weeks (colon26-*PSF1p-EGFP*) after initial inoculation, 100 sorted EGFP$^+$, EGFP^{low}, or EGFP^{high} tumor cells were again transplanted into new hosts. EGFP^{high} cells from both LLC and colon26 tumors formed significantly larger tumors than did EGFP^{low} or EGFP$^+$ cells (Fig. 2B). When tumor cell components were examined in tumors generated after the second transplantation, EGFP^{high} cells were found to have given rise to both EGFP^{high} and EGFP^{low} cells in both LLC and colon26 tumors (Supplementary Fig. S1). Taken together, these data suggest that cancer cells expressing higher levels of *PSF1* exhibit high cloning efficiency and tumorigenicity.

EGFP(PSF1)^{high} cells possess greater invasive and metastatic capacity. We investigated that EGFP^{high} cells also play a crucial role in tumor metastasis. We determined the overall ability of cells sorted, as described in Fig. 1C, for invasion using Matrigel, a basement membrane model used to estimate metastatic potential. EGFP^{high} cells migrated more effectively than did EGFP^{low} cells or EGFP$^+$ cells, indicating that they possess greater invasive capacity (Fig. 3A and B).

Next, we examined the *in vivo* metastatic potential of these cells by two different means. First, viable sorted EGFP^{high} or EGFP^{low} cells from LLC tumors were injected into the tail veins of recipient mice. After 4 weeks, macrometastatic lesions

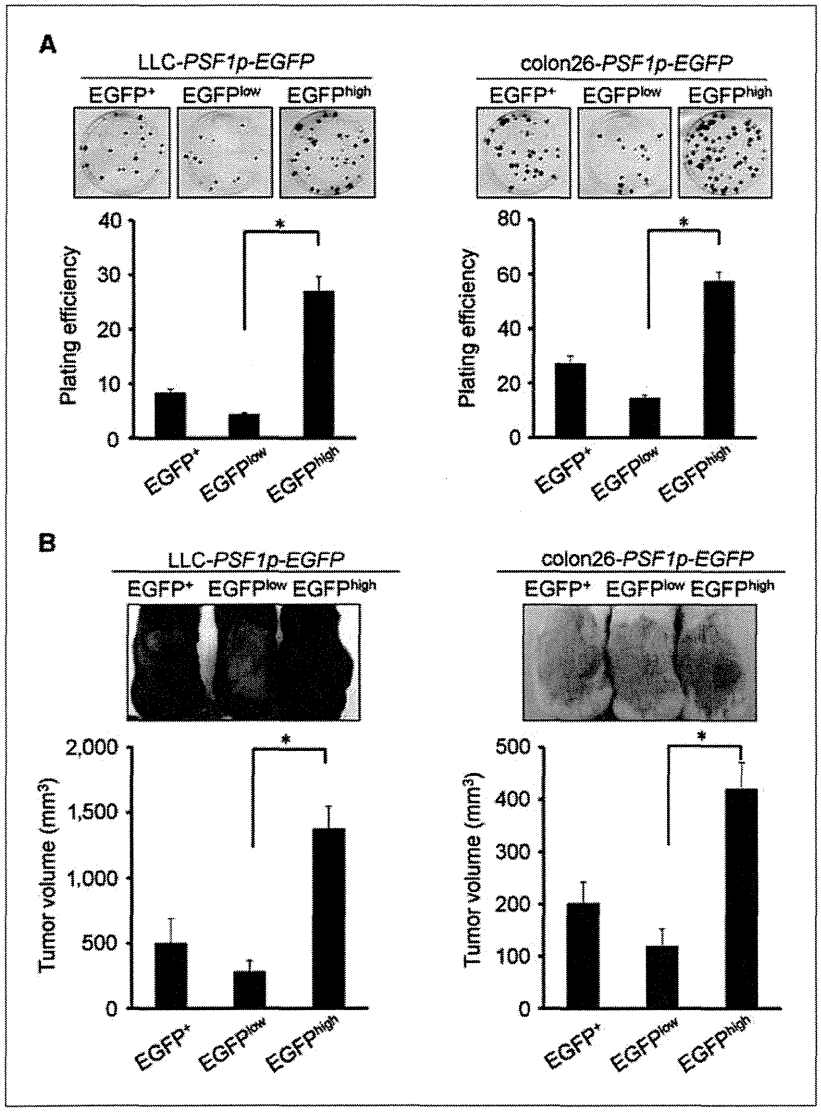

Figure 2. High proliferative ability of PSF1^{high} cancer cells. A, plating efficiency of sorted cells. Sorted cells from tumor tissues injected with LLC-*PSF1p-EGFP* or colon26-*PSF1p-EGFP* were seeded onto 10-cm culture dishes and cultured for 2 wks. Colonies generated from different fractions as indicated were stained with Giemsa solution (top). Quantitative evaluation of colonies from each fraction as indicated. Percentages of the colony numbers relative to the number of cells seeded are presented (bottom). Data show the mean ± SEM. *, $P < 0.01$ ($n = 3$). Results shown are representative of at least three independent experiments. B, tumorigenesis assay. Gross appearance of the tumor mass in mice 5 wks after inoculation with sorted cancer cells as indicated (top). Tumor volume was determined 5 wks after inoculation with sorted cells as indicated (bottom). Data show the mean ± SEM. *, $P < 0.01$ ($n = 10$). Experiments were done at least three times with similar results.

Published OnlineFirst January 26, 2010; DOI: 10.1158/0008-5472.CAN-09-3662

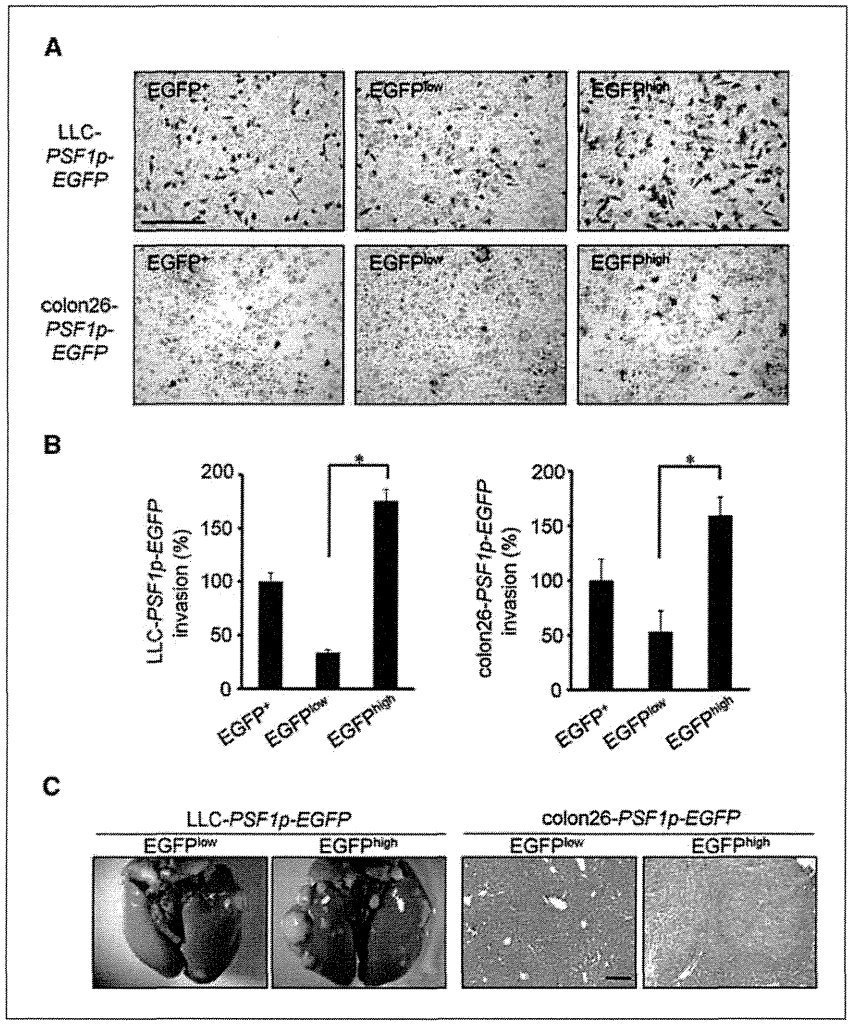

Figure 3. Invasive and metastatic capacity of LLC-*PSF1p-EGFP* and colon26-*PSF1p-EGFP*. A, representative images of sorted cells that migrated across a Matrigel-coated membrane. Bar, 200 μm. B, quantitative evaluation of the migrated cells: percentage of migrated cells relative to the applied total cell number normalized with the data from EGFP$^+$ cells. Data show the mean ± SEM. *, $P < 0.01$ ($n = 3$). Results shown are representative of at least three independent experiments. C, metastasis analysis. Gross appearance of lung metastases after injection with sorted EGFP^{low} or EGFP^{high} cells from LLC tumor (left). Liver metastases after injection with sorted EGFP^{low} or EGFP^{high} cells from colon26 tumor (right). Bar, 200 μm. Results shown are representative of at least three independent experiments.

in the lung were enumerated. Results clearly indicated that EGFP^{high} cells had a higher metastatic potential than did EGFP^{low} cells (Fig. 3C; Supplementary Fig. S2A). Second, in the case of colon26 tumors, viable sorted EGFP^{high} or EGFP^{low} cells were injected into the spleen. After 12 days, metastatic nodules in the liver were analyzed on liver sections. EGFP^{low} cells rarely generated metastatic foci, but large lesions were frequently observed in the livers of mice injected with EGFP^{high} cells (Fig. 3C; Supplementary Fig. S2B).

ESC-like signatures are enriched in EGFP^{high} cells versus EGFPlow cells. Recent studies showed that poor prognosis in a diverse set of human and mouse malignancies is associated with the expression of an ESC-like genetic program (18). We therefore compared the gene expression signatures of EGFP^{low} and EGFP^{high} cells. Data clearly indicated that ESC-like signatures were enriched in EGFP^{high} cells versus EGFP^{low} cells (Fig. 4). Interestingly, other ESC-like signatures (24, 25), in which some cancer-initiating/stem cells (CIC/CSC) were enriched, were also enriched in EGFP^{high} cells versus EGFP^{low} cells (Fig. 4; Supplementary Table S1). Taken together, the results from all the above experiments lead us to conclude that cancer cells harboring large amounts of PSF1 or high transcriptional activity of *PSF1* possess malignant features, including high proliferative capacity, tumorigenesis, metastatic ability, and genetic profiles of poor prognosis.

PSF1^{high} cells are localized in perivascular regions. Next, the tissue distribution of EGFP^{high} cells in tumors was examined (Fig. 5A–C). EGFP^{high} cells were located close to the edge of the tumor and near the blood vessels. Preliminary, we investigated PSF1 expression in human carcinoma specimens (Supplementary Fig. S3). We found that PSF1 expression in human lung and esophageal squamous cell carcinoma specimens was confined to the surrounding basal-like cells and located at some distance from the centers of terminal differentiation zones. Furthermore, PSF1-positive cells were located in close proximity to blood vessels near the edge of the tumor, as observed in our murine xenograft model (Supplementary Fig. S3).

Silencing of PSF1 inhibits the proliferation of carcinoma cells. Targeted disruption of PSF1 led to embryonic lethality

Published OnlineFirst January 26, 2010; DOI: 10.1158/0008-5472.CAN-09-3662

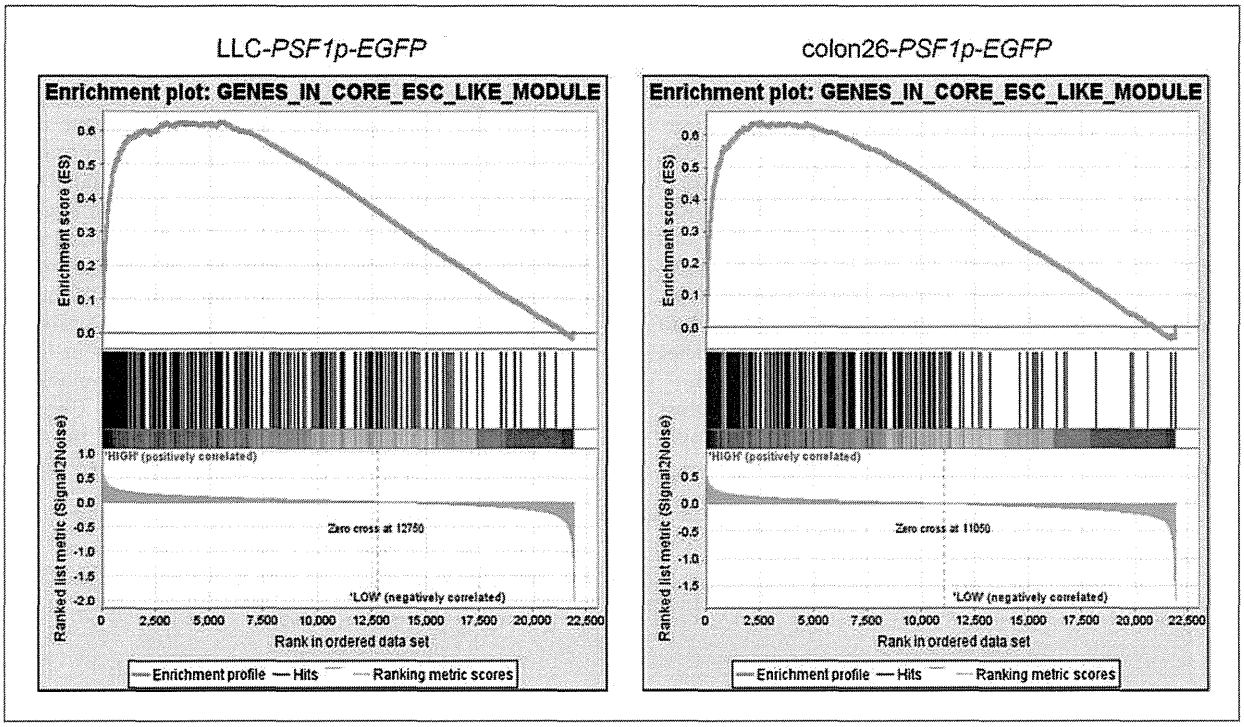

Figure 4. Gene set enrichment analysis. GSEA plots show that expression of an ESC-like core gene module (24) is more enriched in EGFP^{high} cells compared with EGFP^{low} cells in LLC-*PSF1p-EGFP* tumor and colon26-*PSF1p-EGFP* tumor.

caused by the inhibition of cell growth in the inner cell mass (12), suggesting that silencing this gene may also inhibit tumor cell proliferation. To determine whether PSF1 could be a suitable molecular target for anticancer drug development, the inhibitory effects of its expression in human carcinoma cell lines should be evaluated. In budding yeast, it has been suggested that PSF1 plays a role in DNA replication, associated with the formation of the DNA replication fork (7–9). However, its function in mammalian cells has not been clarified. First, we established the cellular localization of PSF1 in HeLa cells (Fig. 6A). At interphase, PSF1 was localized predominantly in the nuclei. During mitosis, it was almost exclusively diffusely located outside the chromatin. Next, we used short hairpin RNA (shRNA) expression plasmids for RNAi-mediated endogenous gene silencing in HeLa cells *in vitro*. Quantitative RT-PCR with gene-specific shRNA confirmed that endogenous PSF1 gene expression was reduced by more than 75% within 72 hours, compared with the lack of effect of transfection of a scrambled shRNA expression plasmid (data not shown). At 96 hours, the total number of PSF1 shRNA–treated cells was significantly decreased compared with the control (Fig. 6B), suggesting that depletion of PSF1 had resulted in cell growth arrest. To analyze more precisely the effect of PSF1 depletion on cell growth, first, the DNA contents were analyzed (Fig. 6C, left). Results showed that depletion of PSF1 led to an increase in the fraction of cells in the sub-G_1, S, and G_2-M phases, suggesting that this molecule is important not only for S phase but also for G_2-M phase progression.

Polyploid cells can arise as a result of errors in mitosis. These cells usually exit the cycle in an aberrant fashion, without sister chromatid segregation or cytokinesis, a process known as "mitotic slippage." Cancer cell lines (such as HeLa and HEK293T cells) lacking functional p53 progress into S phase without p53-dependent growth arrest at the subsequent G_1-S boundary, and hyperploid cells develop as a result. However, no obvious hyperploid cell populations were found in PSF1-depleted cells (Fig. 6C, left). During a 4-hour pulse, approximately 75% of scrambled shRNA–treated cells incorporated BrdUrd (Fig. 6C, right), but only approximately 23% of PSF1-depleted cells possessed large nuclei staining with anti-BrdUrd antibody. Taken together, these data indicate that PSF1 depletion also inhibits DNA synthesis of multiploid cells, which resulted in the generation of only a small number of cells harboring large nuclei (8N; Fig. 6C, left).

During the 72- to 120-hour period after shRNA treatment, the population of G_2-M phase cells increased in the PSF1 depletion experiments (Fig. 6C, left). Therefore, we assessed the function of PSF1 in G_2-M progression. In the scrambled shRNA–treated control population, most cells had divided within 60 minutes, whereas division times were prolonged in the PSF1-depleted cells (Fig. 6D, left). To examine this in terms of chromosome segregation, real-time imaging was done with histone H2B-GFP, which labels the chromosomes (Fig. 6D, middle). In control cells, the chromosomes were condensed and congressed to the metaphase plate, but subsequently, and suddenly, they completely segregated and the

Published OnlineFirst January 26, 2010; DOI: 10.1158/0008-5472.CAN-09-3662

time spent in metaphase was between 15 and 30 minutes. By contrast, PSF1 depletion prolonged the duration of metaphase by between 33 and 145 minutes, and a proportion of the PSF1-depleted cells showed abnormal chromosome congression and segregation (data not shown). Real-time observation with GFP-tubulin also revealed that depletion of PSF1 caused arrest at metaphase (data not shown). To resolve whether this mitotic arrest, induced by PSF1 depletion, was dependent on the spindle assembly checkpoint, Mad2 was co-depleted from the cells. We found that the mitotic arrest of almost all co-depleted cells was rescued by the early onset of anaphase (Fig. 6D, right). Taken together, these data showed that, in the absence of PSF1, the spindle checkpoint signal was activated and mitotic arrest was precipitated.

Because we observed abnormalities in metaphase arrest and DNA segregation in PSF1-depleted cells, we next analyzed spindle organization by staining for β-tubulin. Results showed that approximately 10% of the mitotic cells formed multipolar asters (Fig. 6E, left), whereas a small number of abnormal spindles were found in the control experiments (data not shown). Moreover, by immunostaining with anti-survivin antibody, we found that unaligned chromosomes were present in PSF1 shRNA–treated cells, which may reflect a defect in chromosome congression or segregation (Fig. 6E, middle). Recently, we reported that PSF1-deficient mice were nonviable at around embryonic day E6.5 and that BrdUrd incorporation was inhibited in the cultured inner cell mass from the blastocysts of E3.5 *PSF1*$^{-/-}$ embryos (12). Consistent with the present results from RNAi experiments in HeLa cells, we found that micronuclei and abnormal chromosomal segregation occurred in E3.5 *PSF1*$^{-/-}$ blastocysts (Fig. 6E, right). These data indicate that PSF1 contributes not only

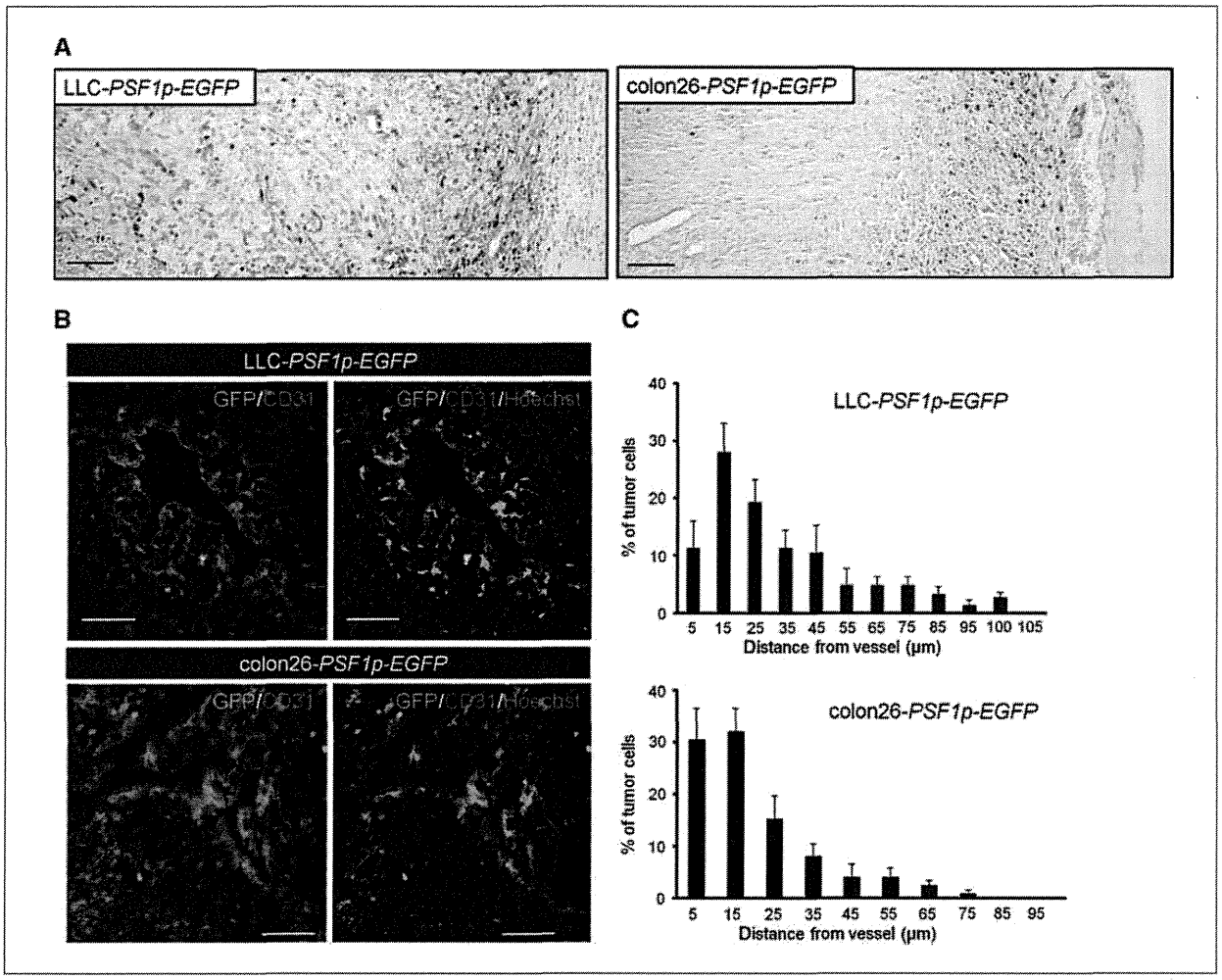

Figure 5. Localization of cancer cells strongly expressing PSF1. A, sections from LLC-*PSF1p-EGFP* (left) and colon26-*PSF1p-EGFP* (right) xenografts were double stained with anti-GFP antibody (brown in left, purple in right) and anti-CD31 antibody (red). Bar, 100 μm. B, sections of LLC-*PSF1p-EGFP* (top) and colon26-*PSF1p-EGFP* (bottom) tumor tissues were stained with anti-CD31 antibody (red). Nuclei were counterstained with Hoechst 33342 (blue). Endogenous EGFP was observed in low contrast (left) and high contrast (right). C, percentages of EGFP^{high} cells that were located at incremental distances of 5 μm from the nearest CD31^{+} endothelial cells. Data are mean ± SEM from five random fields. Bar, 100 μm.

Published OnlineFirst January 26, 2010; DOI: 10.1158/0008-5472.CAN-09-3662

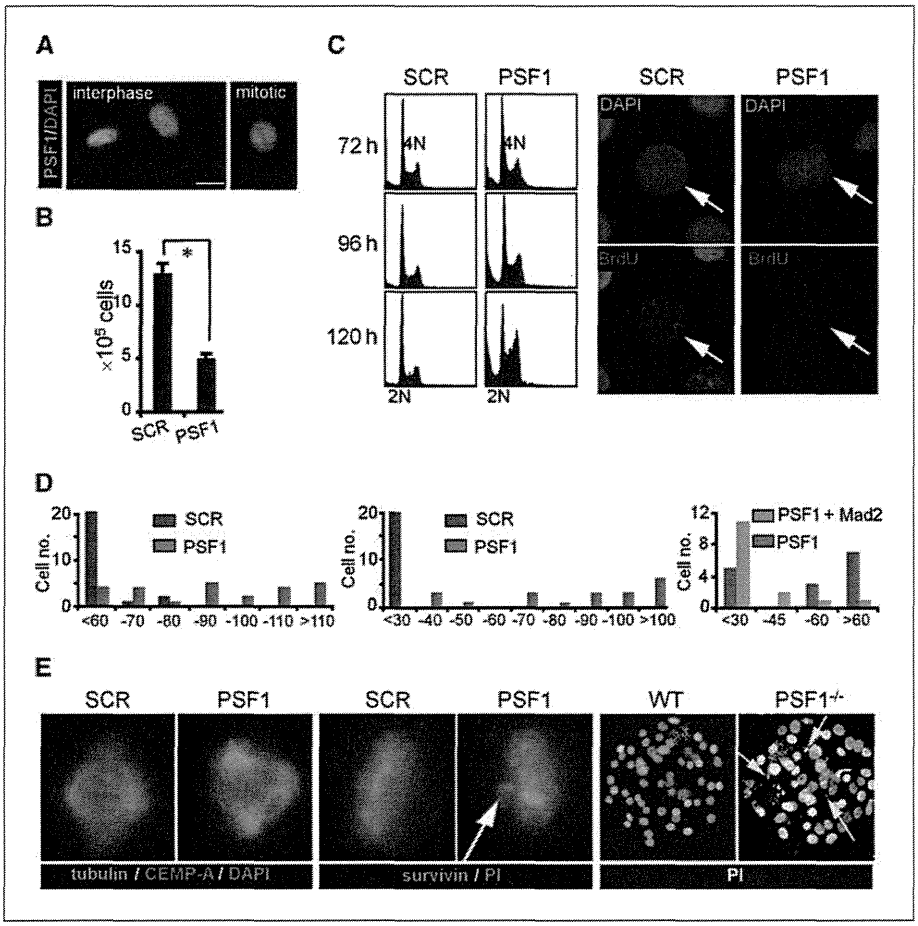

Figure 6. *PSF1* silencing inhibits proliferation of cancer cells. A, HeLa cells were immunostained with anti-PSF1 (green). DNA was counterstained with 4′,6-diamidino-2-phenylindole (DAPI; blue). B, total numbers of RNAi-treated HeLa cells 96 h after transfection (bottom). *SCR*, nonspecific scrambled shRNA as a negative control. *, $P < 0.05$. C, DNA content of shRNA-treated HeLa cells (72 h after transfection) was determined by flow cytometry (left). DNA synthesis in large nucleated cells treated with the indicated shRNA. Immunostaining was done with anti-BrdUrd antibody (red), and counterstaining with DAPI (blue; right). Arrows, large nuclei. D, HeLa cells were treated with control (blue) or PSF1 (red) shRNA. Time required for cell division was evaluated by time-lapse observation 72 to 96 h after transfection (left). Using histone H3-GFP–expressing HEK293T cells, metaphase retention time was observed 72 to 120 h after transfection (middle). The H3-GFP-HEK293T cells were cotransfected with PSF1 shRNA and scrambled shRNA (red) or PSF1 and Mad2 shRNA vectors (green), and metaphase retention time was observed 36 to 72 h after transfection (right). E, HeLa cells transfected with shRNA as indicated. Expression of tubulin (green) and CENP-A (red; left). DNA was counterstained with DAPI (blue). Expression of survivin (green; middle). DNA was counterstained with propidium iodide (red). E3.5 $PSF1^{+/+}$ or $PSF1^{-/-}$ embryos were fixed and stained with propidium iodide (right). Arrows, disorganized micronuclei.

to DNA replication but also to the transition from metaphase to anaphase, as well as to chromosome segregation.

Discussion

In the present work, we used cells with a high level of expression of PSF1 to show that these malignant cancer cells, which are located in the vascular region and at the edge of the tumor, exhibit high tumorigenic and metastatic ability.

Thus far, acquisition of genetic changes affected by epigenetic manipulation and microenvironmental exposure has been suggested to be responsible for tumor progression. When we cultured the tumor cells *in vitro*, we observed that the population consisted of PSF1(EGFP)^{high} and PSF1(EGFP)^{low} fractions. When sorted and separately injected into mice, we failed to detect any marked differences between them in terms of tumorigenic or metastatic capacity (data not shown). When nonfractionated tumor cells from these cultures were injected, the tumors that developed consisted of both PSF1(EGFP)^{high} and PSF1(EGFP)^{low} cells. However, when these cells extracted from tumors *in vivo* were fractionated into PSF1(EGFP)^{high} and PSF1(EGFP)^{low} and injected into mice again, then we did see clear a difference in terms of tumorigenic and metastatic capacity between the two fractions.

Our model therefore strongly supports the possibility that environmental changes *in vivo* clearly affect the features of cancer cells with regard to tumorigenicity or nontumorigenicity. Thus, this model suggested that the interaction of cancer

Published OnlineFirst January 26, 2010; DOI: 10.1158/0008-5472.CAN-09-3662

cells with their microenvironment changes them into more malignant ones. In our tumor model as well as histology of human tissues, cells highly positive for PSF1 are located near blood vessels. It has been suggested that CSCs/CICs localize in the perivascular region (26), as is observed in normal organs, where stem cells are located in the vascular niche (27). Furthermore, microarray data clearly indicated that ESC-like signatures, which are reported to be enriched in CSCs/CICs fractions, were also enriched in $EGFP^{high}$ cells versus $EGFP^{low}$ cells (Fig. 4). Thus, the subpopulation of cells strongly positive for PSF1 might include the CSC/CIC fraction.

Antitumor angiogenesis is a promising approach for managing cancer patients, and many angiogenesis-disrupting agents have been developed (28). Although some agents have already been tested clinically and prolongation of survival has been confirmed, it is impossible to destroy all of the blood vessels in a tumor. Recent research in mice has suggested that the tumor repopulates from the edge region to the center after treatment with an angiogenesis-disrupting agent (28), and also that malignant tumor cells egress through remnant blood vessels at the tumor edge after inhibition of vascular endothelial growth factor signals (29). We previously reported that blood vessels in peripheral regions of tumors are well matured compared with those in the center and that they are resistant to antiangiogenic drugs (19, 30). Our data therefore strongly support the notion that cells with malignant features located near blood vessels at the tumor edge and showing resistance to angiogenesis-disrupting agents are responsible for invasion and metastasis. Our present model represents a precise analytic tool to determine whether candidate drugs directed against cells with malignant features including CSCs/CICs or blood vessels actually do suppress proliferation of cancer cells or destroy the vascular niche.

Our data clearly indicate that PSF1 plays a pivotal role in DNA replication and microtubule organization. Recently, it has been suggested that molecules homologous with those associated with DNA replication in lower species also regulate other cellular events in mammalian cells (31–33). In higher eukaryotes, a number of environmental cues affecting cell division involve DNA replication proteins that are also used by lower eukaryotes and that perform diverse functions in cytokinesis. Therefore, there is a possibility that, in addition to its role in microtubule organization, which we have shown here, plus the known part it plays in DNA replication, PSF1 may also have other cellular functions in symmetrical or asymmetrical cell division of malignant cancer cells by influencing cell structure. As we showed here, the possibility that PSF1 is expressed by malignant cancer cells, which may include CSCs or CICs, and the finding that silencing PSF1 induced cancer cell apoptosis suggest that this molecule may represent an important new target for the development of anticancer drugs.

Disclosure of Potential Conflicts of Interest

No potential conflicts of interest were disclosed.

Acknowledgments

We thank N. Fujimoto and K. Fukuhara for technical assistance, and A. Taguchi for technical assistance with the microarray analysis.

Grant Support

Japanese Ministry of Education, Culture, Sports, Science and Technology and the Japanese Society for Promotion of Science.

The costs of publication of this article were defrayed in part by the payment of page charges. This article must therefore be hereby marked *advertisement* in accordance with 18 U.S.C. Section 1734 solely to indicate this fact.

Received 10/7/09; revised 11/25/09; accepted 12/3/09; published OnlineFirst 1/26/10.

References

1. Takayama Y, Kamimura Y, Okawa M, Muramatsu S, Sugino A, Araki H. GINS, a novel multiprotein complex required for chromosomal DNA replication in budding yeast. Genes Dev 2003;17:1153–65.
2. Bauerschmidt C, Pollok S, Kremmer E, Nasheuer HP, Grosse F. Interactions of human Cdc45 with the Mcm2-7 complex, the GINS complex, and DNA polymerases δ and epsilon during S phase. Genes Cells 2007;12:745–58.
3. Gambus A, Jones RC, Sanchez-Diaz A, et al. GINS maintains association of Cdc45 with MCM in replisome progression complexes at eukaryotic DNA replication forks. Nat Cell Biol 2006;8:358–66.
4. Kanemaki M, Sanchez-Diaz A, Gambus A, Labib K. Functional proteomic identification of DNA replication proteins by induced proteolysis *in vivo*. Nature 2003;423:720–4.
5. Moyer SE, Lewis PW, Botchan MR. Isolation of the Cdc45/Mcm2-7/GINS (CMG) complex, a candidate for the eukaryotic DNA replication fork helicase. Proc Natl Acad Sci U S A 2006;103:10236–41.
6. Pacek M, Tutter AV, Kubota Y, Takisawa H, Walter JC. Localization of MCM2-7, Cdc45, and GINS to the site of DNA unwinding during eukaryotic DNA replication. Mol Cell 2006;21:581–7.
7. Chang YP, Wang G, Bermudez V, Hurwitz J, Chen XS. Crystal structure of the GINS complex and functional insights into its role in DNA replication. Proc Natl Acad Sci U S A 2007;104:12685–90.
8. De Falco M, Ferrari E, De Felice M, Rossi M, Hubscher U, Pisani FM. The human GINS complex binds to and specifically stimulates human DNA polymerase α-primase. EMBO Rep 2007;8:99–103.
9. Kamada K, Kubota Y, Arata T, Shindo Y, Hanaoka F. Structure of the human GINS complex and its assembly and functional interface in replication initiation. Nat Struct Mol Biol 2007;14:388–96.
10. Kubota Y, Takase Y, Komori Y, et al. A novel ring-like complex of *Xenopus* proteins essential for the initiation of DNA replication. Genes Dev 2003;17:1141–52.
11. Barkley LR, Song IY, Zou Y, Vaziri C. Reduced expression of GINS complex members induces hallmarks of pre-malignancy in primary untransformed human cells. Cell Cycle 2009;8:1577–88.
12. Ueno M, Itoh M, Kong L, Sugihara K, Asano M, Takakura N. PSF1 is essential for early embryogenesis in mice. Mol Cell Biol 2005;25:10528–32.
13. Han Y, Ueno M, Nagahama Y, Takakura N. Identification and characterization of stem cell-specific transcription of PSF1 in spermatogenesis. Biochem Biophys Res Commun 2009;380:609–13.
14. Ueno M, Itoh M, Sugihara K, Asano M, Takakura N. Both alleles of

Published OnlineFirst January 26, 2010; DOI: 10.1158/0008-5472.CAN-09-3662

PSF1 are required for maintenance of pool size of immature hematopoietic cells and acute bone marrow regeneration. Blood 2009; 113:555–62.
15. Obama K, Ura K, Satoh S, Nakamura Y, Furukawa Y. Up-regulation of PSF2, a member of the GINS multiprotein complex, in intrahepatic cholangiocarcinoma. Oncol Rep 2005;14:701–6.
16. Hayashi R, Arauchi T, Tategu M, Goto Y, Yoshida K. A combined computational and experimental study on the structure-regulation relationships of putative mammalian DNA replication initiator GINS. Genomics Proteomics Bioinformatics 2006;4:156–64.
17. Ryu B, Kim DS, Deluca AM, Alani RM. Comprehensive expression profiling of tumor cell lines identifies molecular signatures of melanoma progression. PLoS One 2007;2:e594.
18. Ben-Porath I, Thomson MW, Carey VJ, et al. An embryonic stem cell-like gene expression signature in poorly differentiated aggressive human tumors. Nat Genet 2008;40:499–507.
19. Satoh N, Yamada Y, Kinugasa Y, Takakura N. Angiopoietin-1 alters tumor growth by stabilizing blood vessels or by promoting angiogenesis. Cancer Sci 2008;99:2373–9.
20. Kanda T, Sullivan KF, Wahl GM. Histone-GFP fusion protein enables sensitive analysis of chromosome dynamics in living mammalian cells. Curr Biol 1998;8:377–85.
21. Fujita H, Fukuhara S, Sakurai A, et al. Local activation of Rap1 contributes to directional vascular endothelial cell migration accompanied by extension of microtubules on which RAPL, a Rap1-associating molecule, localizes. J Biol Chem 2005;280:5022–31.
22. Fukuhara S, Sako K, Minami T, et al. Differential function of Tie2 at cell-cell contacts and cell-substratum contacts regulated by angiopoietin-1. Nat Cell Biol 2008;10:513–26.
23. Subramanian A, Tamayo P, Mootha VK, et al. Gene set enrichment analysis: a knowledge-based approach for interpreting genome-wide expression profiles. Proc Natl Acad Sci U S A 2005;102:15545–50.
24. Wong DJ, Liu H, Ridky TW, Cassarino D, Segal E, Chang HY. Module map of stem cell genes guides creation of epithelial cancer stem cells. Cell Stem Cell 2008;2:333–44.
25. Somervaille TC, Matheny CJ, Spencer GJ, et al. Hierarchical maintenance of MLL myeloid leukemia stem cells employs a transcriptional program shared with embryonic rather than adult stem cells. Cell Stem Cell 2009;4:129–40.
26. Calabrese C, Poppleton H, Kocak M, et al. A perivascular niche for brain tumor stem cells. Cancer Cell 2007;11:69–82.
27. Kiel MJ, Yilmaz OH, Iwashita T, Terhorst C, Morrison SJ. SLAM family receptors distinguish hematopoietic stem and progenitor cells and reveal endothelial niches for stem cells. Cell 2005;121:1109–21.
28. Tozer GM, Kanthou C, Baguley BC. Disrupting tumour blood vessels. Nat Rev Cancer 2005;5:423–35.
29. Paez-Ribes M, Allen E, Hudock J, et al. Antiangiogenic therapy elicits malignant progression of tumors to increased local invasion and distant metastasis. Cancer Cell 2009;15:220–31.
30. Okamoto R, Ueno M, Yamada Y, et al. Hematopoietic cells regulate the angiogenic switch during tumorigenesis. Blood 2005;105: 2757–63.
31. Kearsey SE, Cotterill S. Enigmatic variations: divergent modes of regulating eukaryotic DNA replication. Mol Cell 2003;12:1067–75.
32. Hemerly AS, Prasanth SG, Siddiqui K, Stillman B. Orc1 controls centriole and centrosome copy number in human cells. Science 2009; 323:789–93.
33. Prasanth SG, Prasanth KV, Stillman B. Orc6 involved in DNA replication, chromosome segregation, and cytokinesis. Science 2002;297: 1026–31.

Published OnlineFirst December 15, 2009; DOI: 10.1158/1078-0432.CCR-09-1204

Clinical Cancer Research

Cancer Therapy: Preclinical

Hepatocyte Growth Factor Reduces Susceptibility to an Irreversible Epidermal Growth Factor Receptor Inhibitor in *EGFR*-T790M Mutant Lung Cancer

Tadaaki Yamada[1], Kunio Matsumoto[2], Wei Wang[1], Qi Li[1], Yasuhiko Nishioka[3], Yoshitaka Sekido[4], Saburo Sone[3], and Seiji Yano[1]

Abstract

Purpose: The secondary T790M mutation in epidermal growth factor receptor (*EGFR*) is the most frequent cause of acquired resistance to the reversible EGFR tyrosine kinase inhibitors (EGFR-TKI), gefitinib and erlotinib, in lung cancer. Irreversible EGFR-TKIs are expected to overcome the reversible EGFR-TKI resistance of lung cancer harboring T790M mutation in *EGFR*. However, it is clear that resistance may also develop to this class of inhibitors. We showed previously that hepatocyte growth factor (HGF) induced gefitinib resistance of lung cancer harboring *EGFR*-activating mutations. Here, we investigated whether HGF induced resistance to the irreversible EGFR-TKI, CL-387,785, in lung cancer cells (H1975) harboring both L858R activating mutation and T790M secondary mutation in *EGFR*.

Experimental Design: CL-387,785 sensitivity and signal transduction in H1975 cells were examined in the presence or absence of HGF or HGF-producing fibroblasts with or without HGF-MET inhibitors.

Results: HGF reduced susceptibility to CL-387,785 in H1975 cells. Western blotting and small interfering RNA analyses indicated that HGF-induced hyposensitivity was mediated by the MET/phosphoinositide 3-kinase/Akt signaling pathway independent of EGFR, ErbB2, ErbB3, and ErbB4. Hyposensitivity of H1975 cells to CL-387,785 was also induced by coculture with high-level HGF-producing lung fibroblasts. The hyposensitivity was abrogated by treatment with anti-HGF neutralizing antibody, HGF antagonist NK4, or MET-TKI.

Conclusions: We showed HGF-mediated hyposensitivity as a novel mechanism of resistance to irreversible EGFR-TKIs. It will be clinically valuable to investigate the involvement of HGF-MET–mediated signaling in *de novo* and acquired resistance to irreversible EGFR-TKIs in lung cancer harboring T790M mutation in *EGFR*. *Clin Cancer Res; 16(1); 174–83. ©2010 AACR.*

Lung cancer is the most common cause of malignancy-related death worldwide and its incidence is still increasing. Non–small cell lung cancer accounts for ~80% of cases of lung cancer. Median survival of metastatic non–small cell lung cancer is 8 to 10 months even if treated with the most active combination of conventional chemotherapeutic agents (1, 2). Epidermal growth factor (EGF) receptor (EGFR)–activating mutations, such as deletion in exon 19 and L858R point mutation in exon 21 (3), were found in non–small cell lung cancer. These mutations are predominantly found in female, nonsmoking, adenocarcinoma patients and in patients of East Asian origin and are associated with favorable response to the reversible EGFR tyrosine kinase inhibitors (EGFR-TKI), gefitinib and erlotinib (4). Several prospective clinical trials showed that 70% to 75% of non–small cell lung cancer patients with tumors harboring these mutations respond to gefitinib or erlotinib (3, 5). However, even patients who show a marked response to initial treatment also develop acquired resistance to the EGFR TKIs almost without exception after varying periods (3).

Several mechanisms, including T790M secondary mutation in *EGFR* (6, 7), *MET* amplification (8), and overexpression of hepatocyte growth factor (HGF; ref. 9), were reported to induce acquired resistance to reversible EGFR-TKI for non–small cell lung cancer with EGFR-activating mutations. The first mechanism of acquired resistance described was acquisition of the T790M *EGFR* mutation. The methionine residue at position 790 generates a bulkier side chain that either affects binding of TKIs or enhances the affinity of the EGFR tyrosine kinase pocket

Authors' Affiliations: Divisions of [1]Medical Oncology and [2]Tumor Dynamics and Regulation, Cancer Research Institute, Kanazawa University, Ishikawa, Japan; [3]Department of Respiratory Medicine & Rheumatology, Institute of Health Biosciences, The University of Tokushima Graduate School, Tokushima, Japan; and [4]Division of Molecular Oncology, Aichi Cancer Center Research Institute, Nagoya, Japan

Note: Supplementary data for this article are available at Clinical Cancer Research Online (http://clincancerres.aacrjournals.org/).

Corresponding Author: Seiji Yano, Division of Medical Oncology, Cancer Research Institute, Kanazawa University, Takaramachi 13-1, Kanazawa-shi, Ishikawa-ken 920-0934, Japan. Phone: 81-76-265-2780; Fax: 81-76-234-4524; E-mail: syano@staff.kanazawa-u.ac.jp.

doi: 10.1158/1078-0432.CCR-09-1204

Published OnlineFirst December 15, 2009; DOI: 10.1158/1078-0432.CCR-09-1204

Translational Relevance

The most frequent cause of acquired resistance to the reversible epidermal growth factor receptor tyrosine kinase inhibitors (EGFR-TKI), gefitinib and erlotinib, in lung cancer is the secondary T790M mutation in EGFR. Irreversible EGFR-TKIs have the potential to be useful in controlling the reversible EGFR-TKI resistance of lung cancer. Although some of these inhibitors are in clinical development and early signs of success have been reported in lung cancer patients who were refractory to the reversible EGFR-TKI, it is clear that resistance may also develop against this class of inhibitors.

In this study, we showed that hepatocyte growth factor (HGF) reduced susceptibility to irreversible EGFR-TKI in lung cancer cells with the secondary T790M mutation in *EGFR*. We further showed that HGF-MET inhibitors could circumvent the HGF-induced hyposensitivity to irreversible EGFR-TKI. Our findings provide a novel insight into the involvement of HGF-MET–mediated signaling in acquired resistance to irreversible EGFR-TKIs in lung cancer harboring T790M mutation in *EGFR*.

to ATP (7), and this enhanced ATP affinity decreases the effective binding of gefitinib and erlotinib to the tyrosine kinase pocket of EGFR (10). T790M in *EGFR* is found most frequently (~50%) in patients with acquired resistance to EGFR-TKI (7, 11). A minor population of clones with this second mutation (T790M) is thought to exist in the tumor before treatment and to be selected and expand during continuous treatment with gefitinib or erlotinib and hence develop a resistant phenotype (3, 12, 13). Resistance mediated by secondary T790M mutation is thought to be manageable by irreversible EGFR inhibitors, such as CL-387,785, PF00299804, HKI-272, and EKB-569, which bind covalently to Cys^{797} of EGFR (14–17). Although some of these inhibitors are in clinical development and early signs of success have been reported in lung cancer patients who were refractory to gefitinib or erlotinib (18–20), it is clear that resistance may also develop against this class of inhibitors.

We recently showed that HGF induces gefitinib resistance in lung cancer harboring EGFR-activating mutation by activating its receptor MET and downstream phosphoinositide 3-kinase (PI3K)/Akt pathway. This mechanism can be involved in both intrinsic resistance and acquired resistance to gefitinib (9). HGF was originally identified as a mitogenic protein for hepatocytes and has been shown to have pleiotropic biological activities (21). HGF and its receptor MET are expressed at various levels in various types of cancer cells, including lung cancer (22–25). A recent study showed that HGF was strongly expressed in 5 of 7 specimens with T790M second mutation obtained from lung cancer patients who developed acquired resistance to gefitinib (26), suggesting that these two resistance mechanisms can coexist in lung cancer patients.

The present study was done to investigate whether HGF induced resistance to irreversible EGFR-TKI in lung cancer cells with secondary T790M mutation in *EGFR*. We assessed this issue using an irreversible EGFR-TKI, CL-387,785, and human lung cancer cells, H1975, harboring both L858R and T790M mutations in *EGFR*. We found that HGF reduced susceptibility to CL-387,785 in H1975 cells by stimulating the MET/Akt pathway. The resistance was also induced by crosstalk to HGF-producing fibroblast cell lines as well as primary cultured fibroblasts established from lung cancer patients. We further showed that HGF-MET inhibitors could circumvent the HGF-induced hyposensitivity to irreversible EGFR-TKI.

Materials and Methods

Cell lines and reagents. The H1975 human lung adenocarcinoma cell line with *EGFR*-L858R/T790M double mutation (10) was kindly provided by Dr. John D. Minna (University of Texas Southwestern Medical Center). The PC-9 and HCC827 human lung adenocarcinoma cell lines with *EGFR*-activating mutation (deletion in exon 19) were purchased from Immuno-Biological Laboratories and American Type Culture Collection, respectively. The MRC-5 lung embryonic fibroblast cell line was obtained from RIKEN Cell Bank. H1975, PC-9, and HCC827 cells were cultured in RPMI 1640 and MRC-5 (P 30-35) cells were cultured in DMEM, supplemented with 10% fetal bovine serum (FBS), penicillin (100 units/mL), and streptomycin (50 μg/mL), in a humidified CO_2 incubator at 37°C. All experiments were done in medium supplemented with 10% FBS.

Gefitinib was obtained from AstraZeneca. Erlotinib hydrochloride was obtained from Roche Pharma. CL-387,785 and SU11274 were purchased from Calbiochem. Cetuximab was purchased from Merck Serono. Recombinant HGF and NK4 were prepared as reported previously (22, 27, 28). The purities of NK4 and HGF were 96.4% and >98%, respectively, as determined by SDS-PAGE and protein staining. Recombinant EGF and insulin-like growth factor-I were obtained from Invitrogen. Transforming growth factor-α (TGF-α) was from BioSource. Goat anti-human HGF neutralizing antibody, monoclonal anti-human EGF neutralizing antibody, goat anti-human TGF-α neutralizing antibody, and control goat IgG were purchased from R&D Systems.

Isolation of fibroblasts from lung cancer tissue. Primary cultured fibroblasts were established from surgically resected tumors from patients with histologically proven lung cancer at Kanazawa University Hospital as described previously (29). The protocol was approved by the Medical Ethical Committee of Kanazawa University. Written informed consent was obtained from all patients. To establish primary fibroblasts, fresh lung cancer tissues from patients were minced with a scalpel in tissue culture dishes, digested with trypsin, and passed though a cell strainer. The resulting suspensions were incubated in

Published OnlineFirst December 15, 2009; DOI: 10.1158/1078-0432.CCR-09-1204

RPMI 1640 supplemented with 10% FBS, penicillin, and streptomycin. After 48 h, unattached cells were removed and the medium was replaced with fresh medium. After 7 to 10 days, the cells formed a homogenous monolayer morphologically consistent with fibroblast-like cells, which were confirmed to consist of >90% type I collagen–positive cells.

Cell proliferation assay. Cell proliferation was measured using the MTT dye reduction method (30). Tumor cells at 80% confluence were harvested, seeded at 2×10^3 per well in 96-well plates, and incubated in RPMI 1640 with 10% FBS. After 24 h of incubation, several concentrations of gefitinib, erlotinib, CL-387,785, goat anti-human HGF neutralizing antibody, control goat IgG, NK4, SU11274, and/or cytokines were added to each well, and incubation was continued for a further 72 h. Then, an aliquot of 50 μL MTT solution (2 mg/mL; Sigma) was added to each well followed by incubation for 2 h at 37°C. The media were removed and the dark blue crystals in each well were dissolved in 100 μL DMSO. Absorbance was measured with a MTP-120 microplate reader (Corona Electric) at test and reference wavelengths of 550 and 630 nm, respectively. The percentage of growth is shown relative to untreated controls. Each experiment was done at least in triplicate and three times independently.

Immunoprecipitation and Western blotting. Tumor cells were incubated in 10 mL RPMI 1640 with 10% FBS in the presence or absence of HGF and/or CL-387,785. Then, cells were washed twice with PBS, harvested in cell lysis buffer [20 mmol/L Tris (pH 7.4), 150 mmol/L NaCl, 1 mmol/L EDTA, 1 mmol/L EGTA, 1% Triton X-100, 2.5 mmol/L sodium pyrophosphate, 1 mmol/L β-glycerophosphate, 1 mmol/L Na_3VO_4, 1 μg/mL leupeptin, and 1 mmol/L phenylmethylsulfonyl fluoride], and flash-frozen on dry ice. After allowing the cells to thaw, the cell lysates were collected with a rubber scraper, sonicated, and centrifuged at 14,000 × *g* (4°C for 20 min). The total protein concentration was measured using a Pierce BCA Protein Assay kit (Pierce). Aliquots of 500 μg total proteins were immunoprecipitated with the appropriate antibodies. Immune complexes were recovered with protein G-Sepharose beads (Zymed Laboratories). For Western blotting assay, immunoprecipitates or cell lysates were subjected to SDS-PAGE (Bio-Rad) and the proteins were then transferred onto polyvinylidene difluoride membranes (Bio-Rad). The membranes were blocked with Blocking One (Nacalai Tesque) for 1 h at room temperature, and the blots were then incubated at 4°C overnight with anti-Met (25H2), anti–phospho-Met (Y1234/Y1235; 3D7), anti-ErbB2 (29D8), anti-ErbB3 (1B2), anti-ErbB4 (111B2), anti–phospho-EGFR (Y1068), anti–phospho-EGFR (Y1086), anti–phospho-ErbB2 ($Tyr^{1221/1222}$; 6B12), anti–phospho-ErbB3 (Tyr^{1289}; 21D3), anti–phospho-ErbB4 (Tyr^{1284}; 21A9), PI3K p85 (19H8), anti-Akt, or anti–phospho-Akt (Ser^{473}) antibodies (1:1,000 dilution; Cell Signaling Technology) and anti-human EGFR (1 μg/mL), anti-human/mouse/rat extracellular signal-regulated kinase 1/2 (ERK1/2; 0.2 μg/mL), or anti–phospho-ERK1/2 (T202/Y204; 0.1 μg/mL) antibodies (R&D Systems). After washing three times, the membranes were incubated for 1 h at room temperature with secondary antibody (horseradish peroxidase–conjugated species-specific antibody). Immunoreactive bands were visualized with SuperSignal West Dura Extended Duration Substrate Enhanced Chemiluminescent Substrate (Pierce). Each experiment was done at least three times independently.

RNA interference. Duplexed Stealth RNA Interference (Invitrogen) against *MET*, *EGFR*, and *ErbB3* and Stealth RNA Interference Negative Control Low GC Duplex 3 (Invitrogen) were used for RNA interference assay. Briefly, aliquots of 1×10^5 H1975 cells in 2 mL antibiotic-free medium were plated on 6-well plates and incubated at 37°C for 24 h. The cells were then transfected with small interfering RNA (siRNA; 250 pmol) or scramble RNA (siSCR) using Lipofectamine 2000 (5 μL) in accordance with the manufacturer's instructions (Invitrogen). After 24 h, the cells were washed twice with PBS and incubated with or without CL-387,785 (300 nmol/L) and/or recombinant human HGF (50 ng/mL) for an additional 72 h in antibiotic-containing medium. These cells were then used for proliferation assay as described above. *MET*, *EGFR*, and *ErbB3* knockdown were confirmed by Western blotting analysis. The sequences of siRNAs were as follows: *MET* 5′-UCCAGAAGAUCAGUUUCCUAAUUCA-3′ and 5′-UGAAUUAGGAAACUGAUCUUCUGGA-5′, *EGFR* 5′-UUUAAAUUCACCAAUACCUAUUCCG-3′ and 5′-CGGAAUAGGUAUUGGUGAAUUUAAA-5′, and *ErbB3* 5′-GGCCAUGAAUGAAUUCUCUACUCUA-3′ and 5′-UAGAGUAGAGAAUUCAUUCAUGGCC-3′. Each experiment was done at least in triplicate and three times independently.

HGF production in cell culture supernatant. Cells (2×10^5) were cultured in 2 mL RPMI 1640 or DMEM with 10% FBS for 24 h. The cells were washed with PBS and incubated for 48 h in RPMI 1640 or DMEM with 10% FBS with or without various concentrations of CL-387,785. The culture medium was then harvested and centrifuged, and the supernatant was stored at -70°C until analysis. For determination of HGF, ELISA was done in accordance with the manufacturer's recommended procedures (Immunis HGF EIA; B-Bridge International). All samples were run in triplicate. Color intensity was measured at 450 nm with a spectrophotometric plate reader. Growth factor concentrations were determined by comparison with standard curves. The detection limit was 0.1 ng/mL.

Coculture of lung cancer cells with fibroblasts. The coculture system was done using Transwell chambers separated by an 8-μm pore size filter. Tumor cells (8×10^3 per 700 μL) with or without CL-387,785 (300 nmol/L) in the bottom chamber were cocultured with fibroblasts (10^4 cells per 300 μL) with or without 2 h of pretreatment with control IgG (2 μg/mL), anti-HGF neutralizing antibody (2 μg/mL), anti-EGF neutralizing antibody (2 μg/mL), or anti-TGF-α neutralizing antibody (2 μg/mL) in the top chamber for 72 h. The top chamber was then removed and 200 μL MTT solution (2 mg/mL; Sigma) was added to each well and the cells were incubated for 2 h at 37°C. The medium was removed and the dark blue crystals in each well

Published OnlineFirst December 15, 2009; DOI: 10.1158/1078-0432.CCR-09-1204

were dissolved in 400 μL DMSO. Absorbance was measured with a MTP-120 microplate reader (Corona Electric) at test and reference wavelengths of 550 and 630 nm, respectively. The percentage of growth is shown relative to untreated controls. Each experiment was done at least in triplicate and three times independently.

Statistical analysis. All data, expressed as mean ± SE, were analyzed by Mann-Whitney *U* test, and $P < 0.05$

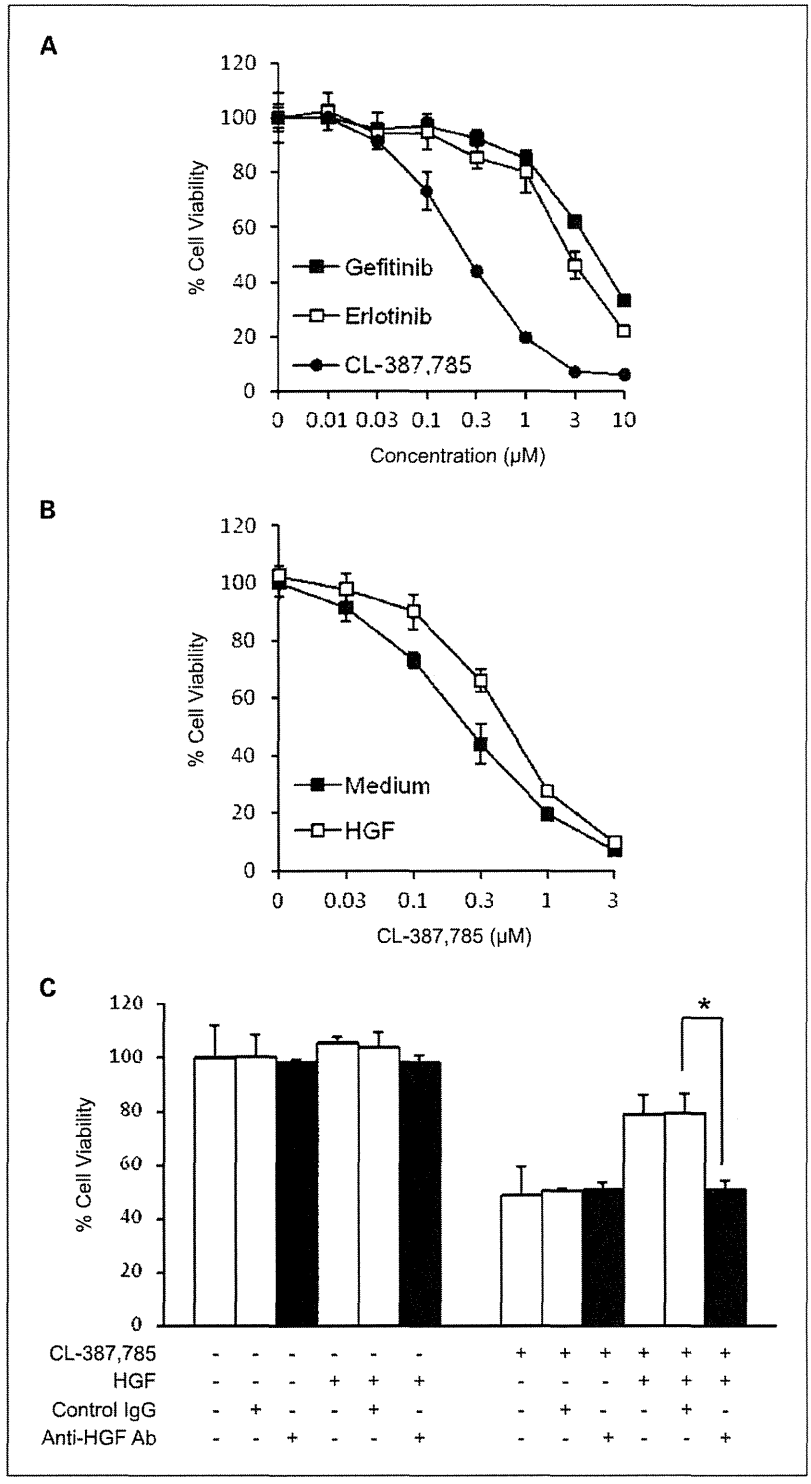

Fig. 1. HGF induced CL-387,785 hyposensitivity of lung adenocarcinoma cells with *EGFR*-L858R/T790M mutations. *A*, H1975 cells were highly sensitive to CL-387,785 (IC_{50} = 300 nmol/L) and resistant to gefitinib and erlotinib. Tumor cells were incubated with increasing concentrations of CL-387,785, gefitinib, or erlotinib and cell growth was determined after 72 h of treatment by MTT assay. *B*, HGF induced CL-387,785 hyposensitivity of H1975 cells with *EGFR*-L858R/T790M mutation. Tumor cells were incubated with increasing concentrations of CL-387,785 and/or HGF at 50 ng/mL, and cell growth was determined in the same way as in *A*. *C*, pretreatment of HGF with anti-HGF antibody abrogated HGF-induced hyposensitivity of H1975 cells to CL-387,785. HGF (50 ng/mL) was pretreated with control IgG (2 μg/mL) or anti-HGF antibody (2 μg/mL) at 37°C for 1 h. The resultant solutions were added to the cultures of tumor cells with or without CL-387,785 (300 nmol/L). Cell growth was determined in the same way as in *A*. *, $P < 0.01$, Mann-Whitney *U* test.

Published OnlineFirst December 15, 2009; DOI: 10.1158/1078-0432.CCR-09-1204

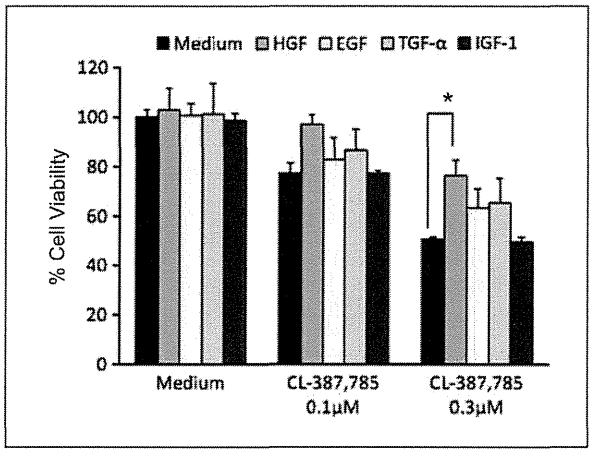

Fig. 2. HGF was most potent in induction of CL-387,785 hyposensitivity of H1975 cells. H1975 cells were incubated with or without CL-387, 785 and/or 50 ng/mL of HGF, EGF, TGF-α, or insulin-like growth factor-I. Cell growth was determined after 72 h of treatment. The percentage of growth is shown relative to untreated controls. *, $P < 0.05$, Mann-Whitney *U* test.

was considered to indicate statistical significance. All statistical analyses were done using StatView version 5.0 (SAS Institute).

Results

HGF induced hyposensitivity to irreversible EGFR-TKI, CL-387,785, in lung cancer cells with EGFR tumor studies. We first examined the effects of the reversible EGFR-TKI, gefitinib and erlotinib, and irreversible EGFR-TKI, CL-387,785, against H1975 cells harboring L858R activating mutation and T790M second mutation in *EGFR* (11). H1975 cells were highly sensitive to CL-387,785 (IC_{50} = 0.24 μmol/L), whereas they were resistant to gefitinib and erlotinib, as reported previously (Fig. 1A; refs. 14, 31). HGF (50 ng/mL) alone had no effect on the proliferation of H1975 cells as well as PC-9 and HCC827 cells with activating mutation in *EGFR*. Under these experimental conditions, HGF (50 ng/mL) reduced the degrees of susceptibility of H1975 (IC_{50} = 0.48 μmol/L), PC-9, and HCC827 cells to CL-387,785 (Fig. 1B; Supplementary Fig. S1). The effect of HGF in H1975 cells was abrogated by anti-HGF neutralizing antibody (2 μg/mL) but not control IgG (2 μg/mL; Fig. 1C).

We also examined the effects of other cytokines, including EGF (32), TGF-α (33), and insulin-like growth factor-I (34), reported to be related to EGFR-TKI sensitivity. Although EGF and TGF-α tended to induce hyposensitivity of H1975 cells to CL-387,785, HGF showed the strongest effect in induction of hyposensitivity to CL-387,785 in H1975 cells (Fig. 2).

HGF-induced CL-387,785 hyposensitivity was mediated by restoring phosphorylation of Akt and ERK1/2 but not EGFR or ErbB3. To investigate the molecular mechanism by which HGF induces CL-387,785 hyposensitivity, we examined the protein expression and phosphorylation status of MET, ErbB family proteins, and downstream molecules by Western blotting. H1975 cells expressed EGFR, ErbB2, ErbB3, ErbB4, MET, and PI3K-P85 proteins. Of these, EGFR, ErbB3, and MET were phosphorylated at various

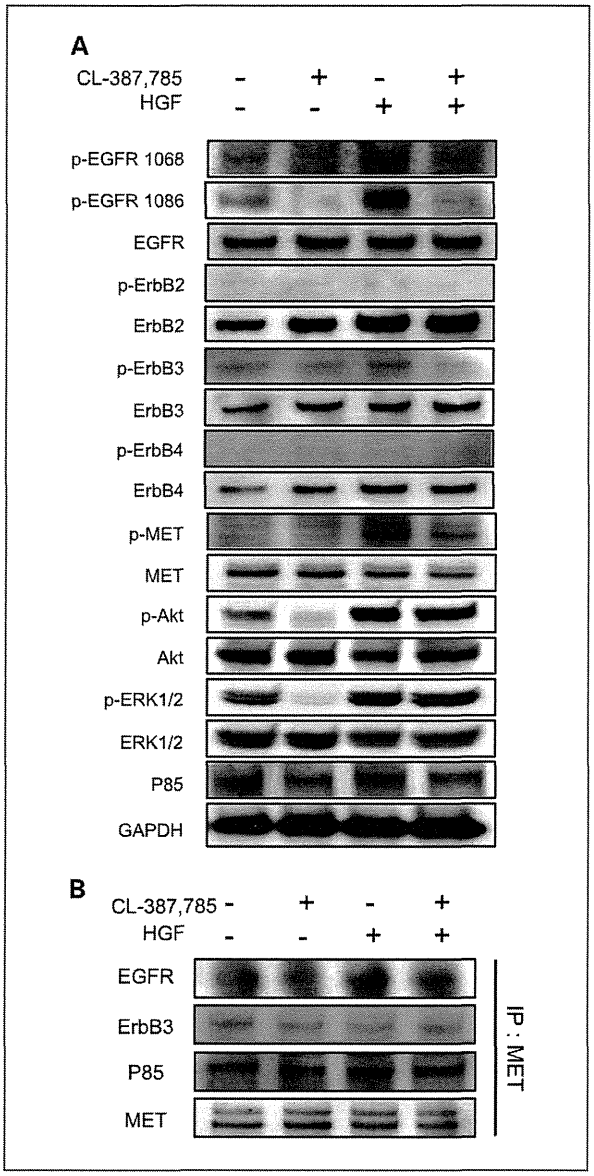

Fig. 3. HGF induces CL-387,785 hyposensitivity of lung adenocarcinoma cells with *EGFR*-T790M mutation by restoring phosphorylation of Akt and ERK1/2 but not EGFR and ErbB3. *A*, CL-387,785 inhibited the phosphorylation of EGFR but did not affect phosphorylation of Akt and ERK1/2 in the presence of HGF. Tumor cells were treated with or without CL-387,785 (300 nmol/L) and/or HGF (50 ng/mL) for 1 h. Cells were lysed and the indicated proteins were detected by immunoblotting. *B*, cell extracts were immunoprecipitated with an antibody to MET. The precipitated proteins were determined by immunoblotting with the indicated antibodies.

Published OnlineFirst December 15, 2009; DOI: 10.1158/1078-0432.CCR-09-1204

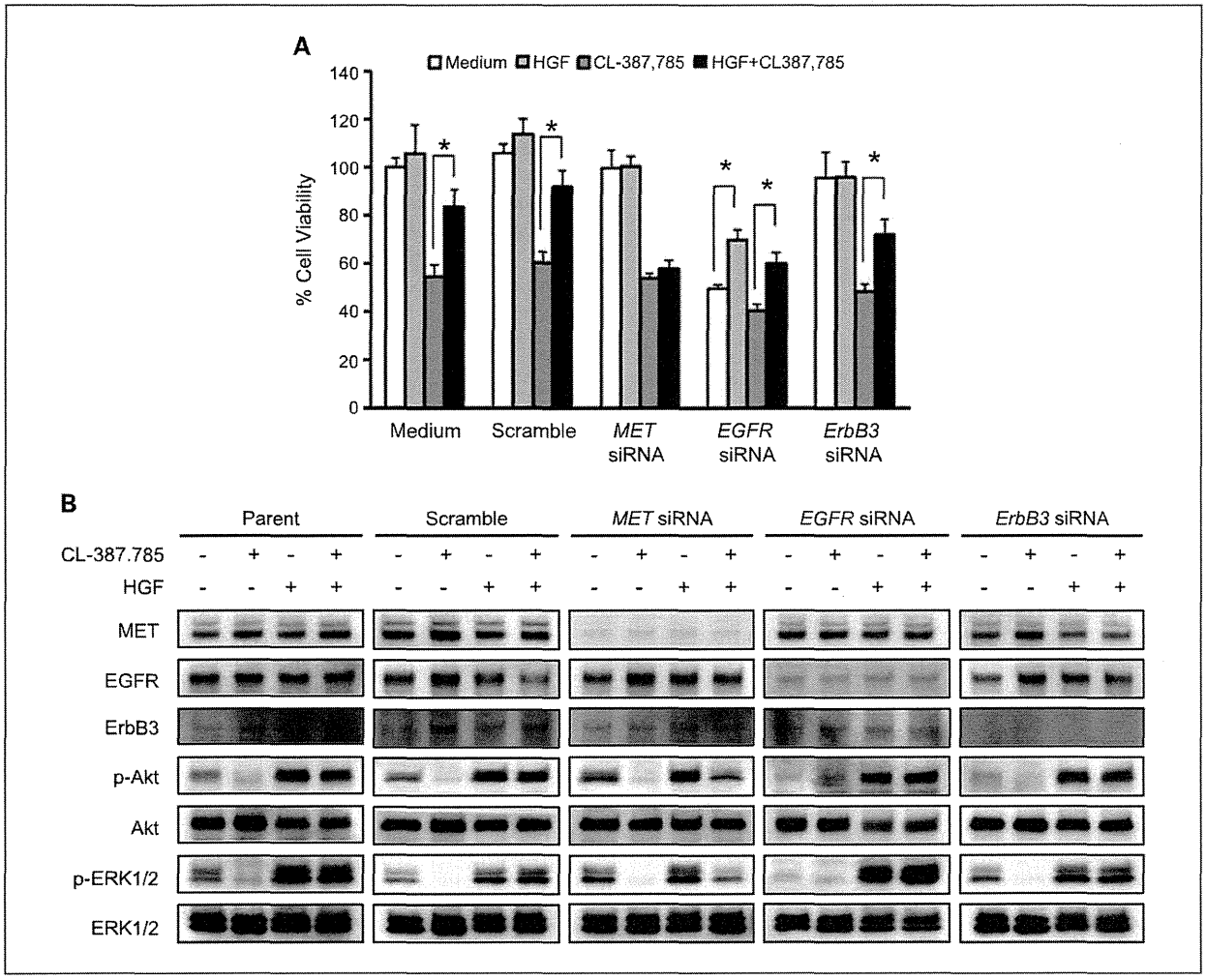

Fig. 4. Specific downregulation of *MET*, but not *EGFR* and *ErbB3*, reversed CL-387,785 hyposensitivity and phosphorylation of Akt and ERK1/2 induced by HGF. *A*, siRNA specific for *MET*, but not for *EGFR* or *ErbB3*, reversed CL-387,785 hyposensitivity by HGF. Control, *MET*-specific, *EGFR*-specific, or *ErbB3*-specific siRNAs were introduced into H1975 cells. The growth of cells with or without CL-387,785 (300 nmol/L) and/or HGF (50 ng/mL) was measured by MTT assay. *, $P < 0.01$, Mann-Whitney *U* test. *B*, downregulation of *MET*, but not *EGFR* and *ErbB3*, by specific-siRNA inhibited restored Akt and ERK1/2 phosphorylation by HGF in cells treated with CL-387,785. Control, *MET*-specific, *EGFR*-specific, or *ErbB3*-specific siRNAs were introduced into H1975 cells. After 48 h, the cells were treated with or without CL-387,785 (300 nmol/L) and/or HGF (50 ng/mL) for 1 h, and cell extracts were prepared and immunoblotted with the indicated antibodies.

levels, but neither ErbB2 nor ErbB4 was phosphorylated in H1975 cells under our experimental conditions. Akt and ERK1/2, the downstream molecules of these receptors, were also phosphorylated. CL-387,785 inhibited the phosphorylation of EGFR, ErbB3, Akt, and ERK1/2, but not MET, showing the selectivity of this compound to the EGFR family. HGF alone stimulated phosphorylation of not only MET, Akt, and ERK1/2 but also EGFR and ErbB3. In the presence of HGF, CL-387,785 inhibited the phosphorylation of EGFR but did not affect phosphorylation of Akt or ERK1/2 (Fig. 3A).

To investigate the mechanism in detail, we immunoprecipitated MET and examined the association with PI3K-related molecules. In H1975 cells, MET was constitutively associated with p85, the binding domain of PI3K, and this association was unaffected by CL-387,785 and/or HGF. MET was slightly associated with ErbB3, and this association was also unaffected by CL-387,785 and/or HGF. On the other hand, MET was constitutively associated with EGFR, and this association was augmented by HGF. Importantly, CL-387,785 disrupted association of MET-EGFR irrespective of the presence or absence of HGF (Fig. 3B). These results suggest that, in the absence of EGFR inhibition, some if not all MET protein is associated with EGFR and HGF stimulates MET-EGFR association and downstream signaling (Akt and ERK1/2). In contrast, in the presence of EGFR inhibition, MET may show reduced association with inactivated EGFR. Therefore, HGF may

Published OnlineFirst December 15, 2009; DOI: 10.1158/1078-0432.CCR-09-1204

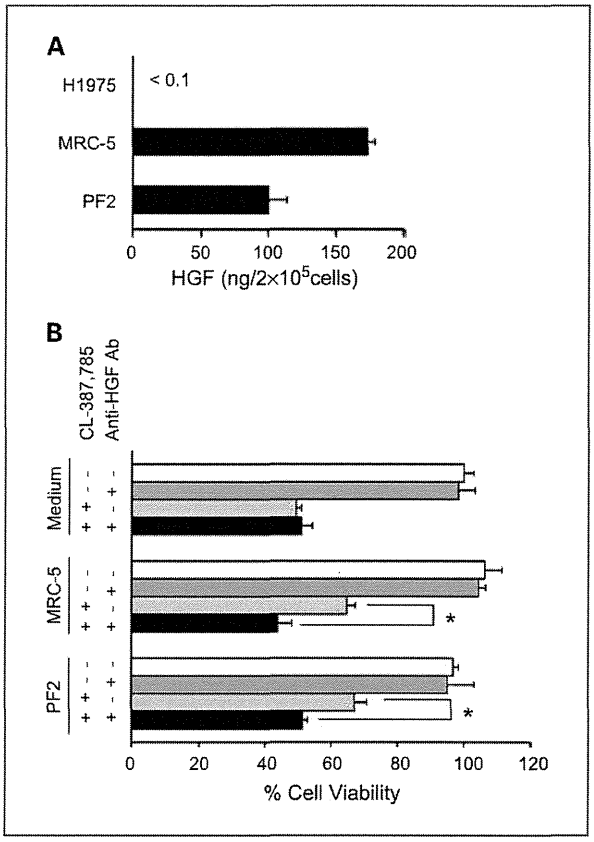

Fig. 5. Fibroblast-derived HGF induces CL-387,785 hyposensitivity in lung cancer cells with *EGFR*-T790M mutations. *A*, HGF production by lung cancer cell line (H1975), human embryonic lung fibroblasts (MRC-5), and primary cultured fibroblasts from the tumor of lung cancer patient 2 (PF2). The cells were incubated in medium for 48 h, the culture supernatants were harvested, and their HGF concentrations were determined by ELISA. *B*, coculture with fibroblasts induced CL-387,785 hyposensitivity in lung cancer cells. The lung cancer H1975 cell line was cocultured with MRC-5 or PF2 cells, with medium, anti-HGF neutralizing antibody (2 μg/mL) in the presence or absence of CL-387,785 (300 nmol/L) for 72 h, and lung cancer cell growth was determined after 72 h of treatment by MTT assay. *, $P < 0.01$, Mann-Whitney *U* test.

stimulate Akt and ERK1/2 signaling predominantly via MET under these conditions.

Specific downregulation of MET, but not EGFR or ErbB3, reversed CL-387,785 hyposensitivity and phosphorylation of Akt and ERK1/2 induced by HGF. To clarify the involvement of MET, EGFR, and ErbB3, we further downregulated *MET*, *EGFR*, and *ErbB3* expression, respectively, with specific siRNAs using H1975 cells. Downregulation of EGFR, but not MET or ErbB3, resulted in reduced viability of H1975 cells, similar to irreversible EGFR-TKI treatment, suggesting the importance of EGFR in viability of H1975 cells. Downregulation of EGFR or ErbB3 did not affect either HGF-induced hyposensitivity to CL-387,785 or phosphorylation of Akt and ERK1/2 restored by HGF in H1975 cells. In parallel experiments, downregulation of MET expression by *MET*-specific siRNA canceled HGF-induced hyposensitivity to CL-387,785 as well as phosphorylation of Akt and ERK1/2 restored by HGF (Fig. 4). These results indicate that HGF induces CL-387,785 hyposensitivity by activating the Akt and ERK1/2 signaling pathway via MET phosphorylation.

Fibroblast-derived HGF induced CL-387,785 hyposensitivity in lung cancer cells. It is well documented that host microenvironments can affect the chemosensitivity of cancers and that stromal fibroblasts are the major source of HGF (35). We next examined the production of HGF by three human fibroblast cell lines and fibroblasts in primary culture established from the tumors of five different lung cancer patients. Our observations indicated that levels of HGF production by these fibroblasts varied and that the human embryonic lung-derived fibroblasts, MRC-5, and the primary culture fibroblasts from patient 2 (PF2) produced high levels of HGF in their supernatants. On the other hand, H1975 cells did not produce detectable levels of HGF in the culture supernatant with or without various concentrations of CL-387,785 (Fig. 5A; Supplementary Fig. S2). To further investigate whether the susceptibility of H1975 cells to CL-387,785 could be affected by crosstalk to stromal fibroblasts, we cocultured the H1975 cells with MRC-5 cells or PF2 using Transwell systems. Whereas H1975 cells were highly sensitive to CL-387,785, exogenously added HGF induced CL-387,785 hyposensitivity of H1975 cells as mentioned above. Coculture with MRC-5 or PF2 cells did not significantly affect the proliferation of H1975 cells. Under these experimental conditions, H1975 cells became hyposensitive to CL-387,785 in the presence of MRC-5 or PF2 cells. This was abrogated by treatment with anti-HGF neutralizing antibody (2 μg/mL) but not the neutralizing antibodies against EGF (2 μg/mL) or TGF-α (2 μg/mL; Fig. 5B; Supplementary Fig. S3). These

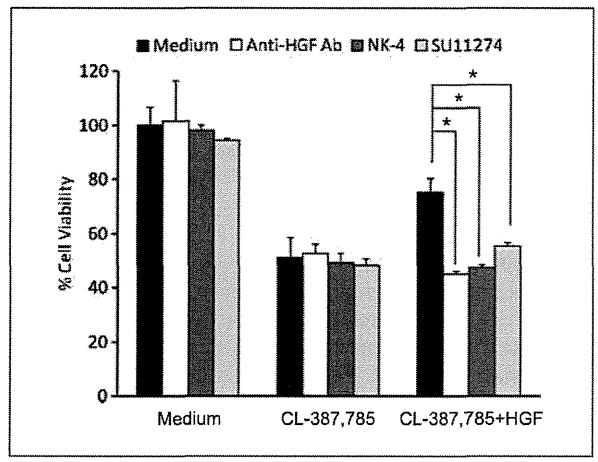

Fig. 6. Anti-HGF antibody, NK4, or SU11274 abrogated HGF-induced CL-387,785 hyposensitivity in lung cancer cells with *EGFR*-T790M mutation. H1975 cells were treated for 72 h with or without CL-387,785 (300 nmol/L) and/or HGF (50 ng/mL) in the presence or absence of anti-HGF neutralizing antibody (2 μg/mL), NK4 (300 nmol/L), or SU11274 (1 μmol/L). Cell growth was determined by MTT assay. *, $P < 0.01$, Mann-Whitney *U* test.

Published OnlineFirst December 15, 2009; DOI: 10.1158/1078-0432.CCR-09-1204

results indicate that fibroblast-derived HGF could induce CL-387,785 hyposensitivity of lung cancer cells with *EGFR*-L858R/T790M mutations.

HGF-induced hyposensitivity was abrogated by addition of HGF-MET inhibitors. Recently, several inhibitors of HGF-MET signaling have been developed. Therefore, to establish the novel therapeutic modality against HGF-mediated resistance to irreversible EGFR-TKI, we treated H1975 cells with CL-387,785 in combination with anti-HGF neutralizing antibody, HGF antagonist, or MET TKI. The MET-TKI, SU11274, moderately reversed the HGF-induced CL-387,785 hyposensitivity at the nontoxic concentration of 1 μmol/L. Both anti-HGF neutralizing antibody (2 μg/mL) and HGF antagonist, NK4 (300 nmol/L), completely abrogated the CL-387,785 hyposensitivity at nontoxic concentrations (Fig. 6), suggesting the promising potential of these compounds to overcome HGF-induced resistance.

Discussion

In the present study, we showed that HGF reduced susceptibility to an irreversible EGFR-TKI, CL-387,785, in human lung cancer cells harboring a secondary T790M mutation. HGF-induced CL-387,785 hyposensitivity was mediated by activation of the PI3K/Akt pathway via phosphorylation of MET independent of EGFR, ErbB2, ErbB3, or ErbB4. The reduced susceptibility was also caused by coculture with an HGF-producing fibroblast cell line as well as primary cultured fibroblasts established from a lung cancer patient. In addition, HGF-MET inhibitors could circumvent the HGF-induced hyposensitivity to irreversible EGFR-TKI.

H1975 is a human lung adenocarcinoma cell line, which has both L858R and T790M as an activating mutation and secondary resistance mutation, respectively, in *EGFR*. This cell line is widely used as a model to develop novel targeting drugs, including irreversible EGFR-TKI, which overcome T790M-mediated drug resistance (14, 15). More recently, this cell line was also used to identify a novel mechanism of resistance to irreversible EGFR-TKI. Yu et al. carried out a cell-based *in vitro* random mutagenesis screen to identify an *EGFR* mutation that induced resistance to CL-387,785 (15). They found several mutations in *EGFR* that induced resistance to CL-387,785 in H1975 cells, although the mechanisms by which these mutations caused resistance remained unclear. In the present study, we showed another mechanism showing that HGF reduced susceptibility to CL-387,785 in this cell line by activating the MET/PI3K/Akt pathway to send a survival signal. In addition, HGF-induced CL-387,785 hyposensitivity was also observed in PC-9 and HCC827 cells, which had *EGFR*-activating mutation (deletion in exon 19) alone. Lung cancer cells with *EGFR*-activating mutations, with or without T790M mutation, seem to be dependent on the signal from the mutated EGFR for their survival (36). Therefore, an alternative signal pathway via MET may be important for their survival when the EGFR signal is blocked by inhibitors. In fact, Tang et al. showed the efficacy of dual receptor tyrosine kinase-targeted inhibition against MET (SU11274) and EGFR (erlotinib or CL-387,785) as a strategy to achieve optimized inhibition in *EGFR*-T790M–mediated erlotinib resistance (37).

To overcome T790M mutation-mediated resistance, several agents, such as irreversible EGFR-TKIs, anti-EGFR antibody (38), and heat shock protein 90 inhibitors (39), have been developed and evaluated with regard to their efficacy in preclinical and clinical trials. Of the irreversible EGFR-TKIs, PF00299804, HKI-272, EKB-569, and BIBW2992 are currently in clinical trials, whereas commercially available CL-387,785 is not (19, 40). Yoshimura et al. reported promising results showing that EKB-569 caused partial responses in two cases of lung cancer that acquired resistance during treatment with reversible EGFR-TKI, gefitinib (18). Other groups also reported early signs of success with HKI-272 and PF00299804 in gefitinib- or erlotinib-refractory cancers (19, 20). Anti-EGFR chimeric antibody, cetuximab, has also been reported to block the downstream signal of EGFR and potently induce antibody-dependent cellular cytotoxicity and thus show antitumor activity against several cell lines, including H1975 (38). However, although these agents show favorable responses in tumors with T790M mutation, it is clear that resistance can also develop against this class of inhibitors. We showed that HGF could induce hyposensitivity to irreversible EGFR-TKI. In addition, our preliminary experiments indicated that although cetuximab inhibited the growth of H1975 cells, HGF caused hyposensitivity to cetuximab (data not shown). Thus, it may be useful to investigate the involvement of HGF-MET–mediated signaling in acquired resistance to irreversible EGFR-TKIs as well as anti-EGFR antibody in lung cancer harboring T790M mutation in *EGFR*.

MET is known to be only one specific receptor for HGF (41, 42). MET activated by HGF binding forms a homodimer and transduces strong signals to various pathways, including PI3K/Akt, mitogen-activated protein kinase/ERK, and STAT (43). MET is also known to form heterodimers with other growth receptors, including EGFR and ErbB3 (8). Engelman et al. reported that amplified MET associated with ErbB3 and caused gefitinib resistance in lung cancer cells (8). Recent reports further indicated the important interaction between MET and EGFR (44, 45). These two receptors mediate collaborative signaling with receptor cross-activation (43). However, direct interaction between MET and EGFR with T790M mutation has not been reported previously. In the present study, we found that MET directly associated with EGFR harboring T790M mutation in H1975 cells and that this association was enhanced by HGF resulting in augmented phosphorylation of Akt and ERK1/2. These observations indicate that MET interacts closely with EGFR harboring T790M mutation and regulates these important signal pathways. Therefore, simultaneous inhibition of MET and EGFR with T790M mutation may be useful not only for overcoming HGF-induced TKI resistance but also for controlling the

Published OnlineFirst December 15, 2009; DOI: 10.1158/1078-0432.CCR-09-1204

progression of TKI-naive tumors with T790M mutation in *EGFR*. Although we could not perform *in vivo* experiments in this study because of the limited availability of CL-387,785, further *in vivo* experiments are warranted to assess the therapeutic effects of irreversible EGFR-TKI combined with HGF-MET inhibitors.

The tumor microenvironment is important for tumor progression and drug sensitivity (46). Fibroblastic stromal cells have been linked to several activities that promote tumor progression, including angiogenesis, epithelial-to-mesenchymal transition, progressive genetic instability, and deregulation of antitumor immune responses, enhanced metastasis, and prevention of apoptosis induced by chemotherapeutic agents. Stromal fibroblasts are one of the major sources of various cytokines, including HGF (35). In the present study, we confirmed that fibroblast cell lines and primary cultured fibroblasts produced various levels of HGF and irreversible EGFR-TKI hyposensitivity could be induced by HGF derived from both fibroblast cell lines and primary cultured fibroblasts by a paracrine mechanism. Therefore, it is possible that tumor-associated fibroblasts are involved in resistance to irreversible EGFR-TKI in lung cancer patients harboring *EGFR*-T790M mutation.

In summary, we reported a novel mechanism of resistance to irreversible EGFR-TKI in lung cancer harboring secondary T790M mutation in *EGFR*. HGF induced hyposensitivity to the irreversible EGFR-TKI, CL-387,785, by activating the PI3K/Akt pathway via phosphorylation of MET independent of EGFR family proteins. The hyposensitivity was also induced by coculture with HGF-producing fibroblasts, suggesting the possible involvement of microenvironments in resistance to irreversible EGFR-TKIs. Moreover, we showed that HGF-MET inhibitors could circumvent the HGF-induced hyposensitivity to irreversible EGFR-TKI. Therefore, it will be clinically valuable to investigate the involvement of HGF-MET–mediated signaling in acquired resistance to irreversible EGFR-TKIs in lung cancer harboring T790M mutation in *EGFR*.

Disclosure of Potential Conflicts of Interest

S. Yano: honoraria, AstraZeneca, Chugai Pharmaceuticals. The other authors disclosed no potential conflicts of interest.

Grant Support

Ministry of Health, Labor, and Welfare of Japan Grant-in-Aid of Cancer Research 16-1 (S. Yano) and Ministry of Education, Science, Sports, and Culture of Japan Grants-in-Aid of Cancer Research 17016051 (S. Sone) and 21390256 (S. Yano).

The costs of publication of this article were defrayed in part by the payment of page charges. This article must therefore be hereby marked *advertisement* in accordance with 18 U.S.C. Section 1734 solely to indicate this fact.

Received 5/14/09; revised 10/13/09; accepted 10/19/09; published OnlineFirst 12/15/09.

References

1. Schiller JH, Harrington D, Belani CP, et al. Comparison of four chemotherapy regimens for advanced non-small-cell lung cancer. N Engl J Med 2002;346:92–8.
2. Ohe Y, Ohashi Y, Kubota K, et al. Randomized phase III study of cisplatin plus irinotecan versus carboplatin plus paclitaxel, cisplatin plus gemcitabine, and cisplatin plus vinorelbine for advanced non-small-cell lung cancer: Four-Arm Cooperative Study in Japan. Ann Oncol 2007;18:317–23.
3. Mitsudomi T, Yatabe Y. Mutations of the epidermal growth factor receptor gene and related genes as determinants of epidermal growth factor receptor tyrosine kinase inhibitors sensitivity in lung cancer. Cancer Sci 2007;98:1817–24.
4. Shigematsu H, Lin L, Takahashi T, et al. Clinical and biological features associated with epidermal growth factor receptor gene mutations in lung cancers. J Natl Cancer Inst 2005;97:339–46.
5. Inoue A, Suzuki T, Fukuhara T, et al. Prospective phase II study of gefitinib for chemotherapy-naive patients with advanced non-small-cell lung cancer with epidermal growth factor receptor gene mutations. J Clin Oncol 2006;24:3340–6.
6. Balak MN, Gong Y, Riely GJ, et al. Novel D761Y and common secondary T790M mutations in epidermal growth factor receptor-mutant lung adenocarcinomas with acquired resistance to kinase inhibitors. Clin Cancer Res 2006;12:6494–501.
7. Kobayashi S, Boggon TJ, Dayaram T, et al. EGFR mutation and resistance of non-small-cell lung cancer to gefitinib. N Engl J Med 2005;352:786–92.
8. Engelman JA, Zejnullahu K, Mitsudomi T, et al. MET amplification leads to gefitinib resistance in lung cancer by activating ERBB3 signaling. Science 2007;316:1039–43.
9. Yano S, Wang W, Li Q, et al. Hepatocyte growth factor induces gefitinib resistance of lung adenocarcinoma with epidermal growth factor receptor-activating mutations. Cancer Res 2008;68:9479–87.
10. Yun CH, Mengwasser KE, Toms AV, et al. The T790M mutation in EGFR kinase causes drug resistance by increasing the affinity for ATP. Proc Natl Acad Sci U S A 2008;105:2070–5.
11. Pao W, Miller VA, Politi KA, et al. Acquired resistance of lung adenocarcinomas to gefitinib or erlotinib is associated with a second mutation in the EGFR kinase domain. PLoS Med 2005;2:225–35.
12. Toyooka S, Kiura K, Mitsudomi T. EGFR mutation and response of lung cancer to gefitinib. N Engl J Med 2005;352:2136.
13. Engelman JA, Mukohara T, Zejnullahu K, et al. Allelic dilution obscures detection of a biologically significant resistance mutation in EGFR-amplified lung cancer. J Clin Invest 2006;116:2695–706.
14. Kobayashi S, Ji H, Yuza Y, et al. An alternative inhibitor overcomes resistance caused by a mutation of the epidermal growth factor receptor. Cancer Res 2005;65:7096–101.
15. Yu Z, Boggon TJ, Kobayashi S, et al. Resistance to an irreversible epidermal growth factor receptor (EGFR) inhibitor in EGFR-mutant lung cancer reveals novel treatment strategies. Cancer Res 2007;67:10417–27.
16. Engelman JA, Zejnullahu K, Gale CM, et al. PF00299804, an irreversible pan-ERBB inhibitor, is effective in lung cancer models with EGFR and ERBB2 mutations that are resistant to gefitinib. Cancer Res 2007;67:11924–32.
17. Kwak EL, Sordella R, Bell DW, et al. Irreversible inhibitors of the EGF receptor may circumvent acquired resistance to gefitinib. Proc Natl Acad Sci U S A 2005;102:7665–70.
18. Yoshimura N, Kudoh S, Kimura T, et al. EKB-569, a new irreversible epidermal growth factor receptor tyrosine kinase inhibitor, with

Published OnlineFirst December 15, 2009; DOI: 10.1158/1078-0432.CCR-09-1204

clinical activity in patients with non-small cell lung cancer with acquired resistance to gefitinib. Lung Cancer 2006;51:363–8.
19. Jänne PA, Schellens JH, Engelman JA, et al. Preliminary activity and safety results from a phase I clinical trial of PF-00299804, an irreversible pan-HER inhibitor, in patients (pts) with NSCLC. J Clin Oncol 2008;26:S20, abstract 8027.
20. Wong KK, Fracasso PM, Bukowski RM, et al. A phase I study with neratinib (HKI-272), an irreversible pan ErbB receptor tyrosine kinase inhibitor, in patients with solid tumors. Clin Cancer Res 2009;15: 2552–8.
21. Nakamura T, Nishizawa T, Hagiya M, et al. Molecular cloning and expression of human hepatocyte growth factor. Nature 1989;342: 440–3.
22. Guo A, Villén J, Kornhauser J, et al. Signaling networks assembled by oncogenic EGFR and c-Met. Proc Natl Acad Sci U S A 2008;105: 692–7.
23. Nakamura Y, Niki T, Goto A, et al. c-Met activation in lung adenocarcinoma tissues: an immunohistochemical analysis. Cancer Sci 2007; 98:1006–13.
24. Masuya D, Huang C, Liu D, et al. The tumour-stromal interaction between intratumoral c-Met and stromal hepatocyte growth factor associated with tumour growth and prognosis in non-small-cell lung cancer patients. Br J Cancer 2004;90:1555–62.
25. Ma PC, Tretiakova MS, MacKinnon AC, et al. Expression and mutational analysis of MET in human solid cancers. Genes Chromosomes Cancer 2008;47:1025–37.
26. Onitsuka T, Uraoto H, Nose N, et al. Acquired resistance to gefitinib: the contribution of mechanisms other than the T790M, MET, and HGF status. Lung Cancer 2009. In press.
27. Seki T, Ihara I, Sugimura A, et al. Isolation and expression of cDNA for different forms of hepatocyte growth factor from human leukocytes. Biochem Biophys Res Commun 1990;172:321–7.
28. Tomioka D, Maehara N, Kuba K, et al. Inhibition of growth, invasion, and metastasis of human pancreatic carcinoma cells by NK4 in an orthotopic mouse model. Cancer Res 2001;61:7518–24.
29. Barker SE, Grosse SM, Siapati EK, et al. Immunotherapy for neuroblastoma using syngeneic fibroblasts transfected with IL-2 and IL-12. Br J Cancer 2007;97:210–7.
30. Green LM, Reade JL, Ware CF. Rapid colorimetric assay for cell viability: application to the quantitation of cytotoxic and growth inhibitory lymphokines. J Immunol Methods 1984;70:257–68.
31. de La Motte Rouge T, Galluzzi L, Olaussen KA, et al. A novel epidermal growth factor receptor inhibitor promotes apoptosis in non-small cell lung cancer cells resistant to erlotinib. Cancer Res 2007;67: 6253–62.
32. Wu W, O'Reilly MS, Langley RR, et al. Expression of epidermal growth factor (EGF)/transforming growth factor-α by human lung cancer cells determines their response to EGF receptor tyrosine kinase inhibition in the lungs of mice. Mol Cancer Ther 2007;6: 2652–63.
33. Ishikawa N, Daigo Y, Takano A, et al. Increases of amphiregulin and transforming growth factor-α in serum as predictors of poor response to gefitinib among patients with advanced non-small cell lung cancers. Cancer Res 2005;65:9176–84.
34. Morgillo F, Kim WY, Kim ES, Ciardiello F, Hong WK, Lee HY. Implication of the insulin-like growth factor-IR pathway in the resistance of non-small cell lung cancer cells to treatment with gefitinib. Clin Cancer Res 2007;13:2795–803.
35. Matsumoto K, Nakamura T. Hepatocyte growth factor and the Met system as a mediator of tumor-stromal interactions. Int J Cancer 2006;119:477–83.
36. Godin-Heymann N, Bryant I, Rivera MN, et al. Oncogenic activity of epidermal growth factor receptor kinase mutant alleles is enhanced by the T790M drug resistance mutation. Cancer Res 2007;67: 7319–26.
37. Tang Z, Du R, Jiang S, et al. Dual MET-EGFR combinatorial inhibition against T790M-EGFR-mediated erlotinib-resistant lung cancer. Br J Cancer 2008;99:911–22.
38. Steiner P, Joynes C, Bassi R, et al. Tumor growth inhibition with cetuximab and chemotherapy in non-small cell lung cancer xenografts expressing wild-type and mutated epidermal growth factor receptor. Clin Cancer Res 2007;13:1540–51.
39. Shimamura T, Li D, Ji H, et al. Hsp90 inhibition suppresses mutant EGFR-T790M signaling and overcomes kinase inhibitor resistance. Cancer Res 2008;68:5827–38.
40. Riely GJ. Second-generation epidermal growth factor receptor tyrosine kinase inhibitors in non-small cell lung cancer. J Thorac Oncol 2008;3:S146–9.
41. Bottaro DP, Rubin JS, Faletto DL, et al. Identification of the hepatocyte growth factor receptor as the c-met proto-oncogene product. Science 1991;251:802–4.
42. Naldini L, Vigna E, Narsimhan RP, et al. Hepatocyte growth factor (HGF) stimulates the tyrosine kinase activity of the receptor encoded by the proto-oncogene c-MET. Oncogene 1991;6:501–4.
43. Boccaccio C, Comoglio PM. Invasive growth: a MET-driven genetic programme for cancer and stem cells. Nat Rev Cancer 2006;6: 637–45.
44. Han C, Michalopoulos GK, Wu T. Prostaglandin E_2 receptor EP1 transactivates EGFR/MET receptor tyrosine kinases and enhances invasiveness in human hepatocellular carcinoma cells. J Cell Physiol 2006;207:261–70.
45. Kubo T, Yamamoto H, Lockwood WW, et al. MET gene amplification or EGFR mutation activate MET in lung cancers untreated with EGFR tyrosine kinase inhibitors. Int J Cancer 2009;124:1778–84.
46. Bhowmick NA, Neilson EG, Moses HL. Stromal fibroblasts in cancer initiation and progression. Nature 2004;432:332–7.

Clin Exp Metastasis (2010) 27:351–359
DOI 10.1007/s10585-010-9333-0

RESEARCH PAPER

Gender difference in bone metastasis of human small cell lung cancer, SBC-5 cells in natural killer-cell depleted severe combined immunodeficient mice

Satoshi Sakaguchi · Hisatsugu Goto · Masaki Hanibuchi · Shinsaku Otsuka · Hirokazu Ogino · Soji Kakiuchi · Hisanori Uehara · Seiji Yano · Yasuhiko Nishioka · Saburo Sone

Received: 28 December 2009 / Accepted: 29 April 2010 / Published online: 13 May 2010

Abstract Lung cancer frequently develops multiple organ metastases, which thus makes this disease a leading cause of malignancy-related death worldwide. A gender difference is reported to affect the incidence and mortality of lung cancer; however, whether and how the gender difference is involved in lung cancer metastasis is unclear. This study evaluated the gender difference in multiple organ metastases in human small cell lung cancer (SBC-5) cells by using natural killer cell-depleted severe combined immunodeficient mice. Among multiple organ metastases, only bone metastasis formation significantly increased in female mice in comparison to males, while no significant difference was observed in the metastases to the liver and lungs. The suppression of androgen by castration or androgen receptor antagonist treatment in male mice also induced a significant increase of bone metastases. The number of osteoclasts in the bone metastatic lesions was greater in female mice and in mice with androgen suppression than in control male. However, there was no significant difference in the serum concentration of parathyroid hormone-related protein (PTHrP) associated with gender or androgen suppression. An in vitro study also indicated that sex steroid treatment had no effect on the proliferation or PTHrP production in SBC-5 cells. These results indicate that the balance of sex steroids therefore plays an important role in the formation of bone metastasis in small cell lung cancer, and suggests diverse mechanisms of interaction between cancer cells and host cells in the bone microenvironment.

Keywords Bicalutamide · Bone metastasis · Castration · Gender difference · Lung cancer · Osteoclast · Sex steroids

S. Sakaguchi and H. Goto contributed equally to this work.

S. Sakaguchi · H. Goto · M. Hanibuchi · S. Otsuka · H. Ogino · Y. Nishioka · S. Sone (✉)
Department of Respiratory Medicine and Rheumatology, Institute of Health Biosciences, The University of Tokushima Gradate School, 3-18-15 Kuramoto-cho Tokushima, Tokushima 770-8503, Japan
e-mail: ssone@clin.med.tokushima-u.ac.jp

S. Kakiuchi · S. Sone
Department of Medical Oncology, Institute of Health Biosciences, The University of Tokushima Gradate School, Tokushima 770-8503, Japan

H. Uehara
Department of Molecular and Environmental Pathology, Institute of Health Biosciences, The University of Tokushima Gradate School, Tokushima 770-8503, Japan

S. Yano
Division of Medical Oncology, Molecular and Cellular Targeting Translational Oncology Center, Cancer Research Institute, Kanazawa University, Kanazawa 920-0934, Japan

Abbreviations

NK	Natural killer
SCID	Severe combined immunodeficient
SCLC	Small cell lung cancer
PTHrP	Parathyroid hormone-related protein
AR	Androgen receptor
ER	Estrogen receptor
NSCLC	Non-small cell lung cancer
DHT	Dehydro-testosterone
E2	β-Estradiol
RT-PCR	Reverse transcription polymerase chain reaction
PCR	Polymerase chain reaction
BSA	Bovine serum albumin
RANK	Receptor activator of nuclear factor-κB
RANKL	Receptor activator of nuclear factor-κB ligand